ETH
Eidgenössische Technische Hochschule Zürich
Swiss Federal Institute of Technology Zurich

Seminar for Applied Mathematics SAM

Higher Order Quasi-Monte Carlo for Bayesian Shape Inversion

R. N. Gantner and M. D. Peters

Research Report No. 2016-42

September 2016
Latest revision: August 2017

Seminar für Angewandte Mathematik
Eidgenössische Technische Hochschule
CH-8092 Zürich
Switzerland

Funding SNF: 149819
Funding: CSCS Project ID d41

Higher Order Quasi-Monte Carlo for Bayesian Shape Inversion*

R. N. Gantner† and M. D. Peters‡

Abstract. In this article, we consider a Bayesian approach towards data assimilation and uncertainty quantification in diffusion problems on random domains. We provide a rigorous analysis of parametric regularity of the posterior distribution given that the data exhibit only limited smoothness. Moreover, we present a dimension truncation analysis for the forward problem, which is formulated in terms of the domain mapping method. Having these novel results at hand, we shall consider as a practical example Electrical Impedance Tomography in the regime of constant conductivities. We are interested in computing moments, in particular expectation and variance, of the contour of an unknown inclusion, given perturbed surface measurements. By casting the forward problem into the framework of elliptic diffusion problems on random domains, we can directly apply the presented analysis. This straightforwardly yields parametric regularity results for the system response and for the posterior measure, facilitating the application of higher order quadrature methods for the approximation of moments of quantities of interest. As an example of such a quadrature method, we consider here recently developed higher order quasi-Monte Carlo methods. To solve the forward problem numerically, we employ a fast boundary integral solver. Numerical examples are provided to illustrate the presented approach and validate the theoretical findings.

Key words. Quasi-Monte Carlo methods, uncertainty quantification, error estimates, high dimensional quadrature, Electrical Impedance Tomography

AMS subject classifications. 65N21, 65N38, 65D30

1. Introduction.

The present article considers the Bayesian approach, see e.g. [13, 15, 48], to assimilate measured data in the framework of elliptic diffusion equations on random domains. The forward problem is solved by means of the domain mapping method as it has been considered in [8, 33, 53]. In particular, we extend here the analysis presented in [33] and consider the impact of dimension truncation on the system response. In view of the computation of quantities of interest, the Bayesian approach boils down to the approximation of high-dimensional integrals. In order to apply the higher order quasi-Monte Carlo methods considered in [17, 27], we provide additionally a rigorous and general analysis of the posterior measure, for a uniform prior and additive Gaussian noise, in the regime where the system response provides only limited smoothness. This might occur in the present setting if the given data, like loadings and boundary data, exhibit only limited regularity. The presented analysis might be considered as an extension of previous works, see particularly [15, 33]. Having these prerequisites at hand, we shall consider Electrical Impedance Tomography (EIT) as a practical example. EIT is a non-invasive medical imaging procedure and has been extensively studied

*Submitted to the editors September 27, 2016.

Funding: This work was supported by the Swiss National Science Foundation (SNSF) under Grant No. SNF149819 to Christoph Schwab and by CPU time from the Swiss National Supercomputing Centre (CSCS) under project ID d41.

†ETH Zurich, Seminar for Applied Mathematics, Rämistrasse 101, CH-8092 Zurich, Switzerland (robert.gantner@sam.math.ethz.ch).

‡University of Basel, Department of Mathematics and Computer Science, Spiegelgasse 1, CH-4051 Basel, Switzerland (michael.peters@unibas.ch).

in the context of inverse problems, see e.g. [2, 3, 20, 21, 34]. Exploiting differences in the electrical conductivity among different biological tissues, EIT reconstructs and images these conductivities based on surface electrode measurements. In particular, we refer here to the case of constant conductivities, where the goal is to determine the shape of an unknown inclusion, see e.g. [7, 9, 30, 34, 39]. Especially in the absence of noise, it is possible to reconstruct the inclusion from a single pair of current/voltage measurements, cf. [7]. This is in contrast to the recent work [19], which also considers Bayesian inversion in the context of EIT. There, the authors reconstruct a diffusion coefficient (representing varying conductivities) from noisy measurements, instead of the shape of the domain.

Our goal will be to approximate the expected shape of an inclusion, given surface measurements from the domain's boundary. The Bayesian framework will allow also arbitrary moments to be computed, allowing specification of a "confidence interval" for the inclusion's shape. A major advantage of the model problem under consideration is that it can be efficiently solved by means of boundary integral equations as it has been done for example in [20]. This allows for numerical studies concerning the convergence behaviour of the applied higher order quasi-Monte Carlo quadrature.

The remainder of this article is structured as follows. In Section 2, we introduce the Bayesian formulation in a rather abstract fashion and parametric regularity results for the posterior measure are derived, given a general regularity estimate for the system response of the forward problem. After this, in Section 3, we present the forward model under consideration, i.e. diffusion problems on random domains, and provide an analysis for the impact of dimension truncation. Section 4 deals with the EIT problem and recasts it into the framework of a diffusion problem on a random domain. We comment also on the discretization by means of boundary integral equations. Interlaced polynomial lattice rules are briefly discussed in the subsequent Section 5, which are the higher-order quasi-Monte Carlo (HoQMC) methods we will use in the computations. In Section 6, a numerical experiment is formulated to compare HoQMC to conventional methods and the results are discussed.

2. Bayesian Inversion.

2.1. The Bayesian Framework. Let $\mathcal{X}$ denote some real and separable Banach space and let $\mathcal{A}(\boldsymbol{y})\colon \mathcal{X} \to \mathcal{X}^*$ be a bounded linear operator for each given parameter sequence $\boldsymbol{y} \in U := [-1/2, 1/2]^{\mathbb{N}}$. For $f(\boldsymbol{y}) \in \mathcal{X}^*$, we consider the parameteric operator equation

$$\mathcal{A}(\boldsymbol{y})q(\boldsymbol{y}) = f(\boldsymbol{y}). \tag{1}$$

We require that the system response q satisfies then a regularity estimate of the form

$$\|\partial_{\boldsymbol{y}}^{\boldsymbol{\nu}} q(\boldsymbol{y})\|_{\mathcal{X}} \leq C|\boldsymbol{\nu}|! c^{|\boldsymbol{\nu}|}\boldsymbol{\gamma}^{\boldsymbol{\nu}} \quad \text{for all } \boldsymbol{\nu} \in \mathcal{F}_{\boldsymbol{\alpha}}, \tag{2}$$

where we denote by $C, c > 0$ constants which are independent of the sequence $\boldsymbol{\nu}$ and $\boldsymbol{\gamma} \in \ell^p(\mathbb{N})$ for $p < 1$, and we use the convention $\boldsymbol{\gamma}^{\boldsymbol{\nu}} := \prod_{k\geq 1} \gamma_k^{\nu_k}$. The set $\mathcal{F}_{\boldsymbol{\alpha}}$ is given by

$$\mathcal{F}_{\boldsymbol{\alpha}} := \{\boldsymbol{\nu} \in \mathbb{N}_0^{\mathbb{N}} : \boldsymbol{\nu} \leq \boldsymbol{\alpha}\}, \quad \text{where } \boldsymbol{\alpha} \in \mathcal{F} := \left\{\boldsymbol{\nu} \in \mathbb{N}_0^{\mathbb{N}} : \sum_{k\geq 1} \nu_k < \infty\right\},$$

i.e. $\mathcal{F}_{\boldsymbol{\alpha}}$ is the set of all finitely supported index sequences that are bounded by $\boldsymbol{\alpha} \in \mathcal{F}$. Typically, such operator equations emerge from diffusion problems with random data, as random diffusion coefficients or right hand sides, see e.g. [6, 11], or even random domains [33].

Since there exists an $s \in \mathbb{N}$ such that $\nu_k = 0$ for all $k > s$ for all $\boldsymbol{\nu} \in \mathcal{F}_{\boldsymbol{\alpha}}$, we shall identify index sequences with multi indices $\boldsymbol{\nu} = [\nu_1, \dots, \nu_s] \in \mathbb{N}_0^s$ without further notice.

Throughout what follows, we will assume the components of $\boldsymbol{y}$ to be stochastically independent and identically uniformly distributed, i.e. we endow the set U with the structure of a probability space with respect to the product measure

$$\mu_0(\mathrm{d}\boldsymbol{y}) = \prod_{k\geq 1} \mathrm{d}y_k.$$

This measure will be referred to as the *prior measure*. We denote by

$$G\colon U \to \mathcal{X}, \quad \boldsymbol{y} \mapsto q(\boldsymbol{y})$$

the *uncertainty-to-solution map*, which maps a given instance $\boldsymbol{y} \in U$ of the parameter sequence to the corresponding solution $q(\boldsymbol{y}) \in \mathcal{X}$.

In forward uncertainty quantification, the goal is to compute the expectation, with respect to the prior measure μ_0, of a quantity of interest (QoI) $\phi\colon \mathcal{X} \to \mathcal{Z}$, where $\mathcal{Z}$ is a Banach space, which is usually assumed to be a continuous linear functional of the parametric solution $q(\boldsymbol{y})$. The goal of Bayesian inverse uncertainty quantification as in [13] is to incorporate noisy measurements of solutions to (14), after potentially incomplete observations. This is modeled by first considering a bounded, linear observation operator $\mathcal{O} \in \mathcal{L}(\mathcal{X}, Y)$ for a Banach space Y, which models e.g. point evaluation of the system response q, or averaging over a certain subdomain. In the following, we assume $Y = \mathbb{R}^K$ with $K < \infty$, i.e. we assume only finitely many measurements of the system response. Then, we define the *uncertainty-to-observation mapping* $\mathcal{G}$ by

$$\mathcal{G} = \mathcal{O} \circ G\colon U \to Y, \quad \boldsymbol{y} \mapsto \mathcal{G}(\boldsymbol{y}) = \mathcal{O}\big(q(\boldsymbol{y})\big). \tag{3}$$

The measured data δ is modeled as resulting from an observation by $\mathcal{O}$, perturbed with additive Gaussian noise, $\delta = \mathcal{O}\big(q(\boldsymbol{y}^\star)\big) + \eta$, where $\boldsymbol{y}^\star$ is the unknown, exact parameter, and $\eta \sim \mathcal{N}(0, \Gamma)$. Hereby, we assume Γ to be a known symmetric, positive definite covariance matrix $\Gamma \in \mathbb{R}^{K\times K}$.

The goal will then be to predict the expectation of the quantity of interest ϕ, which in general is an arbitrary continuous functional of the solution. In particular, it needs not contain the observation operator, thus allowing prediction of "unobservable" phenomena, given perturbed measurements of observable output. To that end, we define the Gaussian potential, also referred to as the least-squares or data misfit functional, by $\Phi_\Gamma\colon U \times Y \to \mathbb{R}$,

$$\Phi_\Gamma(\boldsymbol{y}, \delta) := \frac{1}{2}\|\delta - \mathcal{G}(\boldsymbol{y})\|_\Gamma^2 = \frac{1}{2}\big(\delta - \mathcal{G}(\boldsymbol{y})\big)^\intercal \Gamma^{-1}\big(\delta - \mathcal{G}(\boldsymbol{y})\big). \tag{4}$$

Given the prior measure μ_0, Bayes' formula yields an expression for a *posterior measure* μ^δ on U, given the data δ.

Theorem 1. *Assume that the potential $\Phi_\Gamma\colon U\times Y\to\mathbb{R}$ is μ_0-measurable for $\delta\in Y$. Then the conditional distribution of $\boldsymbol{y}$ given δ, denoted by $\boldsymbol{y}|\delta$, exists and is denoted by μ^δ. It is absolutely continuous with respect to μ_0 and its Radon-Nikodym derivative is given by*

$$\frac{d\mu^\delta}{d\mu_0}(\boldsymbol{y}) = \frac{1}{Z}\exp\big(-\Phi_\Gamma(\boldsymbol{y},\delta)\big), \tag{5}$$

with $Z := \int_U \exp\big(-\Phi_\Gamma(\boldsymbol{y},\delta)\big)\,\mu_0(\mathrm{d}\boldsymbol{y}) > 0$.

Proof. See e.g. [13]. ∎

The goal of computation is thus to approximate the posterior expectation $\mathbb{E}^{\mu^\delta}[\phi(q)] = Z'/Z$, where Z is given in Theorem 1 and

$$Z' := \int_U \phi\big(q(\boldsymbol{y})\big)\exp\big(-\Phi_\Gamma(\boldsymbol{y},\delta)\big)\,\mu_0(\mathrm{d}\boldsymbol{y}). \tag{6}$$

The numerical approximation of $\mathbb{E}^{\mu^\delta}[\phi(q)]$ will consist of three parts:

(i) truncation of the infinite-parametric problem (1) to $s>0$ parameters $\boldsymbol{y}^{(s)} = [y_1,\dots,y_s]^\intercal \in U^{(s)} := [-1/2,1/2]^s$,

(ii) approximation of the solution $q^{(s)}\big(\boldsymbol{y}^{(s)}\big)$ to the dimensionally truncated problem by a solution $q_h^{(s)}\big(\boldsymbol{y}^{(s)}\big)$ obtained using a suitable discretization, and

(iii) approximation of the resulting s-dimensional integral over $\boldsymbol{y}^{(s)}\in U^{(s)}$.

For the latter, instead of resorting to Markov Chain Monte Carlo (MCMC) methods which converge at a (low) rate of $N^{-1/2}$ in the number of evaluations N of the forward model [38], we will adopt a direct, deterministic approach similar to [10, 48] and considered in the form used here for linear, affine-parametric problems in [15, 16]. To that end, we have to provide parametric regularity estimates for the posterior measure, which will be provided in the following subsection.

2.2. Parametric regularity of the posterior. As stated above, it is well known that the system response q satisfies in relevant applications a parametric regularity estimate of the form (2). Therefore, we will take this estimate as a starting point for our analysis.

In view of Lemma 20 from the Appendix, we obtain the following straightforward result.

Lemma 2. *Assume that the solution $q(\boldsymbol{y})$ to an operator equation of the form (1) satisfies (2) with $\boldsymbol{\gamma}\in\ell^p(\mathbb{N})$ for $p<1$. Then the system response q satisfies the decay estimate*

$$\|\partial_{\boldsymbol{y}}^{\boldsymbol{\nu}} q(\boldsymbol{y})\|_{\mathcal{X}} \le \frac{C}{1-c_{\boldsymbol{\lambda}}}\boldsymbol{\nu}!c^{|\boldsymbol{\nu}|}\widetilde{\boldsymbol{\gamma}}^{\boldsymbol{\nu}} \quad \text{for all } \boldsymbol{\nu}\in\mathcal{F}_{\boldsymbol{\alpha}}.$$

where $\widetilde{\gamma}_k := \gamma_k/\lambda_k$ with a positive sequence $\boldsymbol{\lambda}\in\ell^1(\mathbb{N})$ and $c_{\boldsymbol{\lambda}} := \|\boldsymbol{\lambda}\|_{\ell^1(\mathbb{N})} < 1$.

This means that, given a sufficiently fast decay of the sequence $\boldsymbol{\gamma}$, we can always replace the factor $|\boldsymbol{\nu}|!$ by $\boldsymbol{\nu}!$ due to modifying $\boldsymbol{\gamma}$ by an ℓ^1-sequence, e.g. $\big\{k^{-1-\varepsilon}/\widetilde{c}\big\}_k$ for arbitrary $\varepsilon>0$ and a normalization constant $\widetilde{c}>0$.

Now, let $\mathcal{O}\in\mathcal{L}(\mathcal{X};\mathbb{R}^K)$ and let $\mathcal{G}(\boldsymbol{y})$ be defined as in (3). We want to analyze the behavior of the density

$$\exp\big(-\Phi_\Gamma(\boldsymbol{y},\delta)\big),$$

where the functional $\Phi_\Gamma(\boldsymbol{y},\delta)$ is given by (4). Since $\mathcal{O}$ is linear and bounded, we have

$$\big\|\partial_{\boldsymbol{y}}^{\boldsymbol{\nu}}\mathcal{O}\big(q(\boldsymbol{y})\big)\big\|_{\mathbb{R}^K} = \big\|\mathcal{O}\big(\partial_{\boldsymbol{y}}^{\boldsymbol{\nu}}q(\boldsymbol{y})\big)\big\|_{\mathbb{R}^K} \le \|\mathcal{O}\|_{\mathcal{L}(\mathcal{X};\mathbb{R}^K)} C|\boldsymbol{\nu}|!c^{|\boldsymbol{\nu}|}\boldsymbol{\gamma}^{\boldsymbol{\nu}} \quad \text{for all } \boldsymbol{\nu}\in\mathcal{F}_{\boldsymbol{\alpha}}. \tag{7}$$

For the sake of simplicity let Γ be the identity matrix. Then, we start by considering

$$\partial_{\mathbf{x}}^{\boldsymbol{\nu}'} \exp\Big(-\frac{1}{2}\mathbf{x}^\intercal\mathbf{x}\Big).$$

In the univariate case, we know that

$$\partial_x^{\nu'} \exp\Big(-\frac{1}{2}x^2\Big) = (-1)^{\nu'}\exp\Big(-\frac{1}{2}x^2\Big)H_{\nu'}(x),$$

where $H_{\nu'}$ is the probabilists' Hermite polynomial of degree ν'. By a tensor product argument, we obtain

$$\partial_{\mathbf{x}}^{\boldsymbol{\nu}'} \exp\Big(-\frac{1}{2}\mathbf{x}^\intercal\mathbf{x}\Big) = (-1)^{|\boldsymbol{\nu}'|}\exp\Big(-\frac{1}{2}\mathbf{x}^\intercal\mathbf{x}\Big)H_{\boldsymbol{\nu}'}(\mathbf{x}).$$

Herein, the tensor product Hermite polynomial is given by

$$H_{\boldsymbol{\nu}'}(\mathbf{x}) := H_{\nu_1'}(x_1)\cdots H_{\nu_K'}(x_K).$$

Since the Hermite polynomials satisfy

$$|H_{\nu'}(x)| \le c_H \exp\Big(\frac{x^2}{4}\Big)\sqrt{\nu'!} \quad \text{with } c_H := 1.0865,$$

cp. [1, (22.5.18), (22.14.17)], we have the following bound on the derivatives of the multivariate squared exponential function:

$$\Big|\partial_{\mathbf{x}}^{\boldsymbol{\nu}'} \exp\Big(-\frac{1}{2}\mathbf{x}^\intercal\mathbf{x}\Big)\Big| \le c_H^K\sqrt{\boldsymbol{\nu}'!}.$$

Now, consider the affine transform $\mathbf{x}\mapsto\Gamma^{-1/2}(\delta-\mathbf{x})$, then we achieve the bound

$$\Big|\partial_{\mathbf{x}}^{\boldsymbol{\nu}'} \exp\Big(-\frac{1}{2}(\delta-\mathbf{x})^\intercal\Gamma^{-1}(\delta-\mathbf{x})\Big)\Big| \le c_H^K\sqrt{\boldsymbol{\nu}'!}\|\Gamma\|_2^{-\frac{|\boldsymbol{\nu}'|}{2}}.$$

In particular, this implies that

$$\Psi(\mathbf{x}) := \exp\big(-1/2(\delta-\mathbf{x})^\intercal\Gamma^{-1}(\delta-\mathbf{x})\big)$$

is an entire function on $\mathbb{R}^K$, since it is the composition of an affine mapping with the entire squared exponential function. We make use of the following result from [12].

Theorem 3. *Let $f(\mathbf{x})\colon\mathbb{R}^K\to\mathbb{R}$ be an entire function and $g^{(i)}\in C^{\boldsymbol{\alpha}}\big(U\big)$ for $i=1,\dots,K$. Then, the derivatives of $h(\boldsymbol{y}) := f\big(g^{(1)}(\boldsymbol{y}),\dots,g^{(K)}(\boldsymbol{y})\big)\colon U\to\mathbb{R}$ are given according to*

$$\partial_{\boldsymbol{y}}^{\boldsymbol{\nu}}h(\boldsymbol{y}) = \boldsymbol{\nu}!\sum_{1\le|\boldsymbol{\nu}'|}\frac{\partial_{\mathbf{x}}^{\boldsymbol{\nu}'}f(\mathbf{x})|_{\mathbf{x}=\mathbf{0}}}{\boldsymbol{\nu}'!}\sum_{s(\boldsymbol{\nu},\boldsymbol{\nu}')}\prod_{i=1}^{K}\prod_{j=1}^{\nu_i'}\frac{\partial_{\boldsymbol{y}}^{\boldsymbol{\mu}_j^{(i)}}g^{(i)}(\boldsymbol{y})}{\boldsymbol{\mu}_j^{(i)}!} \quad \textit{for all } \boldsymbol{\nu}\in\mathcal{F}_{\boldsymbol{\alpha}}. \tag{8}$$

Herein, the set $s(\boldsymbol{\nu},\boldsymbol{\nu}')$ is defined as

$$s(\boldsymbol{\nu},\boldsymbol{\nu}') := \left\{ \left(\boldsymbol{\mu}_1^{(1)},\dots,\boldsymbol{\mu}_{\nu_1'}^{(1)},\dots,\boldsymbol{\mu}_1^{(K)},\dots,\boldsymbol{\mu}_{\nu_K'}^{(K)}\right) : \boldsymbol{\mu}_j^{(i)} \in \mathcal{F} \text{ and } \sum_{i=1}^{K}\sum_{j=1}^{\nu_i'} \boldsymbol{\mu}_j^{(i)} = \boldsymbol{\nu} \right\}.$$

Proof. See [12] for a proof of this statement. ∎

Combining this estimate with the bound (7), gives the main result of this section.

Theorem 4. *Given that $\boldsymbol{\gamma} \in \ell^p(\mathbb{N})$ for $p < 1/2$, the derivatives of $\exp\big(-\Phi_\Gamma(\boldsymbol{y},\delta)\big)$ can be bounded according to*

$$\left|\partial_{\boldsymbol{y}}^{\boldsymbol{\nu}} \exp\big(-\Phi_\Gamma(\boldsymbol{y},\delta)\big)\right| \le C(\Gamma,\boldsymbol{\lambda},\mathcal{O})^K |\boldsymbol{\nu}|! (2c)^{|\boldsymbol{\nu}|} \widetilde{\boldsymbol{\gamma}}^{\boldsymbol{\nu}} \quad \text{for all } \boldsymbol{\nu} \in \mathcal{F}_{\boldsymbol{\alpha}},$$

where $\widetilde{\gamma}_k := \gamma_k/\lambda_k$ with a positive sequence $\boldsymbol{\lambda} \in \ell^1(\mathbb{N})$, $c_{\boldsymbol{\lambda}} := \|\boldsymbol{\lambda}\|_{\ell^1(\mathbb{N})} < 1$, and $C(\Gamma,\boldsymbol{\lambda},\mathcal{O}) > 0$ is a constant.

Proof. From Lemma 2 and estimate (7), we derive that

$$\left\|\partial_{\boldsymbol{y}}^{\boldsymbol{\nu}} \mathcal{G}(\boldsymbol{y})\right\|_{\mathbb{R}^K} \le C(\boldsymbol{\lambda},\mathcal{O}) \boldsymbol{\nu}! c^{|\boldsymbol{\nu}|} \widetilde{\boldsymbol{\gamma}}^{\boldsymbol{\nu}} \quad \text{for all } \boldsymbol{\nu} \in \mathcal{F}_{\boldsymbol{\alpha}},$$

where $C(\boldsymbol{\lambda},\mathcal{O}) := C\|\mathcal{O}\|_{\mathcal{L}(\mathcal{X};\mathbb{R}^K)}/(1-c_{\boldsymbol{\lambda}})$.

Now, the application of Theorem 3 gives us, cp. (8),

$$\partial_{\boldsymbol{y}}^{\boldsymbol{\nu}} \exp\big(-\Phi_\Gamma(\boldsymbol{y},\delta)\big) = \boldsymbol{\nu}! \sum_{1\le|\boldsymbol{\nu}'|} \frac{\partial_{\mathbf{x}}^{\boldsymbol{\nu}'}\Psi(\mathbf{x})|_{\mathbf{x}=\mathbf{0}}}{\boldsymbol{\nu}'!} \sum_{s(\boldsymbol{\nu},\boldsymbol{\nu}')} \prod_{i=1}^{K}\prod_{j=1}^{\nu_i'} \frac{\partial_{\boldsymbol{y}}^{\boldsymbol{\mu}_j^{(i)}} \mathcal{G}^{(i)}(\boldsymbol{y})}{\boldsymbol{\mu}_j^{(i)}!}.$$

We estimate

$$\begin{aligned}
\left|\partial_{\boldsymbol{y}}^{\boldsymbol{\nu}} \exp\big(-\Phi_\Gamma(\boldsymbol{y},\delta)\big)\right| &\le \boldsymbol{\nu}! \sum_{1\le|\boldsymbol{\nu}'|} \frac{\left|\partial_{\mathbf{x}}^{\boldsymbol{\nu}'}\Psi(\mathbf{x})|_{\mathbf{x}=\mathbf{0}}\right|}{\boldsymbol{\nu}'!} \sum_{s(\boldsymbol{\nu},\boldsymbol{\nu}')} \prod_{i=1}^{K}\prod_{j=1}^{\nu_i'} \frac{\left|\partial_{\boldsymbol{y}}^{\boldsymbol{\mu}_j^{(i)}} \mathcal{G}^{(i)}(\boldsymbol{y})\right|}{\boldsymbol{\mu}_j^{(i)}!} \\
&\le \boldsymbol{\nu}! \sum_{1\le|\boldsymbol{\nu}'|} \frac{c_H^K \|\Gamma\|_2^{-\frac{|\boldsymbol{\nu}'|}{2}}}{\sqrt{\boldsymbol{\nu}'!}} \sum_{s(\boldsymbol{\nu},\boldsymbol{\nu}')} \prod_{i=1}^{K}\prod_{j=1}^{\nu_i'} \frac{C(\boldsymbol{\nu},\mathcal{O}) \boldsymbol{\mu}_j^{(i)}! c^{|\boldsymbol{\mu}_j^{(i)}|} \widetilde{\boldsymbol{\gamma}}^{\boldsymbol{\mu}_j^{(i)}}}{\boldsymbol{\mu}_j^{(i)}!} \\
&\le \boldsymbol{\nu}! c^{|\boldsymbol{\nu}|} \widetilde{\boldsymbol{\gamma}}^{\boldsymbol{\nu}} \sum_{1\le|\boldsymbol{\nu}'|} \frac{c_H^K \|\Gamma\|_2^{-\frac{|\boldsymbol{\nu}'|}{2}}}{\sqrt{\boldsymbol{\nu}'!}} C(\boldsymbol{\nu},\mathcal{O})^{|\boldsymbol{\nu}'|} \sum_{s(\boldsymbol{\nu},\boldsymbol{\nu}')} 1.
\end{aligned}$$

Thus, it remains to estimate the cardinality of the set $s(\boldsymbol{\nu},\boldsymbol{\nu}')$. The number of weak integer compositions for ν_k of length $|\boldsymbol{\nu}'|$ is given according to, see e.g. [35],

$$\left|\left\{\left(\mu_1,\dots,\mu_{|\boldsymbol{\nu}'|}\right) : \mu_i \in \mathbb{N}_0 \text{ and } \mu_1+\dots+\mu_{|\boldsymbol{\nu}'|} = \nu_k\right\}\right| = \binom{\nu_k + |\boldsymbol{\nu}'| - 1}{|\boldsymbol{\nu}'| - 1}.$$

By multiplying the number of possible compositions in each component, we can determine the cardinality of the set $s(\boldsymbol{\nu},\boldsymbol{\nu}')$ by

$$|s(\boldsymbol{\nu},\boldsymbol{\nu}')| = \prod_{k=1}^{s} \binom{\nu_k + |\boldsymbol{\nu}'| - 1}{|\boldsymbol{\nu}'| - 1}.$$

We may bound this cardinality due to the estimate obtained by Lemma 22, i.e.

$$\prod_{k=1}^{s}\binom{\nu_k+|\boldsymbol{\nu}'|-1}{|\boldsymbol{\nu}'|-1}\leq\frac{|\boldsymbol{\nu}|!}{\boldsymbol{\nu}!}\binom{|\boldsymbol{\nu}|+|\boldsymbol{\nu}'|-1}{|\boldsymbol{\nu}'|-1}\leq\frac{|\boldsymbol{\nu}|!}{\boldsymbol{\nu}!}2^{|\boldsymbol{\nu}|+|\boldsymbol{\nu}'|}.$$

Therefore, we arrive at

$$\big|\partial_{\boldsymbol{y}}^{\boldsymbol{\nu}}\exp\big(-\Phi_\Gamma(\boldsymbol{y},\delta)\big)\big|\leq|\boldsymbol{\nu}|!(2c)^{|\boldsymbol{\nu}|}\widetilde{\boldsymbol{\gamma}}^{\boldsymbol{\nu}}\sum_{1\leq|\boldsymbol{\nu}'|}\frac{c_H^K\|\Gamma\|_2^{-\frac{|\boldsymbol{\nu}'|}{2}}}{\sqrt{\boldsymbol{\nu}'!}}\big(2C(\boldsymbol{\lambda},\mathcal{O})\big)^{|\boldsymbol{\nu}'|}.$$

Obviously, the series

$$\sum_{\boldsymbol{\nu}_i'=0}^{\infty}\frac{c_H\|\Gamma\|_2^{-\frac{\boldsymbol{\nu}_i'}{2}}}{\sqrt{\boldsymbol{\nu}_i'!}}\big(2C(\boldsymbol{\lambda},\mathcal{O})\big)^{\boldsymbol{\nu}_i'}$$

is absolutely convergent with respect to each particular direction $\boldsymbol{\nu}_i'$. We denote its limit by $C(\Gamma,\boldsymbol{\lambda},\mathcal{O})$. Hence, by taking the product of this limit with respect to the K components of $\boldsymbol{\nu}'$, we arrive at the assertion. ∎

The following corollary establishes a regularity result similar to Theorem 4 for the entire integrand in (6), i.e.

$$\phi\big(q(\boldsymbol{y})\big)\exp\big(-\Phi_\Gamma(\boldsymbol{y},\delta)\big),$$

under the condition that $\phi\big(q(\boldsymbol{y})\big)\in\mathcal{Z}$ satisfies a regularity estimate similar to (2). Such an estimate holds for example if $\phi\colon\mathcal{X}\to\mathbb{R}$ is a continuous linear functional.

Corollary 5. *Let the quantity of interest $\phi\big(q(\boldsymbol{y})\big)\in\mathcal{Z}$ satisfy a regularity estimate similar to (2), i.e.*

$$\big\|\partial_{\boldsymbol{y}}^{\boldsymbol{\nu}}\phi\big(q(\boldsymbol{y})\big)\big\|_{\mathcal{Z}}\leq\tilde{C}|\boldsymbol{\nu}|!\tilde{c}^{|\boldsymbol{\nu}|}\boldsymbol{\gamma}^{\boldsymbol{\nu}}\quad\text{for all }\boldsymbol{\nu}\in\mathcal{F}_{\boldsymbol{\alpha}}\tag{9}$$

with some constants $\tilde{C},\tilde{c}>0$. Then, there holds

$$\big\|\big[\partial_{\boldsymbol{y}}^{\boldsymbol{\nu}}\big[\phi\big(q(\boldsymbol{y})\big)\exp\big(-\Phi_\Gamma(\boldsymbol{y},\delta)\big)\big]\big\|_{\mathcal{Z}}\leq\hat{C}(|\boldsymbol{\nu}|+1)!\hat{c}^{|\boldsymbol{\nu}|}\widetilde{\boldsymbol{\gamma}}^{\boldsymbol{\nu}}\quad\text{for all }\boldsymbol{\nu}\in\mathcal{F}_{\boldsymbol{\alpha}}$$

with some constants $\hat{C},\hat{c}>0$.

Proof. The application of the Leibniz rule for differentiation gives

$$\partial_{\boldsymbol{y}}^{\boldsymbol{\nu}}\big[\phi\big(q(\boldsymbol{y})\big)\exp\big(-\Phi_\Gamma(\boldsymbol{y},\delta)\big)\big]=\sum_{\boldsymbol{\nu}'\leq\boldsymbol{\nu}}\binom{\boldsymbol{\nu}}{\boldsymbol{\nu}'}\partial_{\boldsymbol{y}}^{\boldsymbol{\nu}'}\phi\big(q(\boldsymbol{y})\big)\partial_{\boldsymbol{y}}^{\boldsymbol{\nu}-\boldsymbol{\nu}'}\exp\big(-\Phi_\Gamma(\boldsymbol{y},\delta)\big)$$

for all $\boldsymbol{\nu}\in\mathcal{F}_{\boldsymbol{\alpha}}$. Therefore, we infer by the triangle inequality

$$\big\|\big[\partial_{\boldsymbol{y}}^{\boldsymbol{\nu}}\big[\phi\big(q(\boldsymbol{y})\big)\exp\big(-\Phi_\Gamma(\boldsymbol{y},\delta)\big)\big]\big\|_{\mathcal{Z}}\leq\sum_{\boldsymbol{\nu}'\leq\boldsymbol{\nu}}\binom{\boldsymbol{\nu}}{\boldsymbol{\nu}'}\big\|\partial_{\boldsymbol{y}}^{\boldsymbol{\nu}'}\phi\big(q(\boldsymbol{y})\big)\big\|_{\mathcal{Z}}\big|\partial_{\boldsymbol{y}}^{\boldsymbol{\nu}-\boldsymbol{\nu}'}\exp\big(-\Phi_\Gamma(\boldsymbol{y},\delta)\big)\big|.$$

Now, the application of Theorem 4 and (9) results in

$$\begin{aligned}
&\big\| \big[\partial_{\boldsymbol{y}}^{\boldsymbol{\nu}} \big[\phi\big(q(\boldsymbol{y})\big) \exp\big(-\Phi_\Gamma(\boldsymbol{y},\delta)\big)\big]\big] \big\|_{\mathcal{Z}} \\
&\quad \le \sum_{\boldsymbol{\nu}' \le \boldsymbol{\nu}} \binom{\boldsymbol{\nu}}{\boldsymbol{\nu}'} \tilde{C} |\boldsymbol{\nu}'|! \tilde{c}^{|\boldsymbol{\nu}'|} \boldsymbol{\gamma}^{\boldsymbol{\nu}'} C(\Gamma, \boldsymbol{\lambda}, \mathcal{O})^K |\boldsymbol{\nu} - \boldsymbol{\nu}'|! (2c)^{|\boldsymbol{\nu}-\boldsymbol{\nu}'|} \widetilde{\boldsymbol{\gamma}}^{\boldsymbol{\nu}-\boldsymbol{\nu}'} \\
&\quad \le \max\big\{\tilde{C}, C(\Gamma, \boldsymbol{\lambda}, \mathcal{O})^K\big\} (\max\{\tilde{c}, 2c\})^{|\boldsymbol{\nu}|} \widetilde{\boldsymbol{\gamma}}^{\boldsymbol{\nu}} \sum_{\boldsymbol{\nu}' \le \boldsymbol{\nu}} \binom{\boldsymbol{\nu}}{\boldsymbol{\nu}'} |\boldsymbol{\nu}'|! |\boldsymbol{\nu} - \boldsymbol{\nu}'|!,
\end{aligned}$$

where we exploited that $\gamma_k \le \tilde{\gamma}_k$ for all $k \in \mathbb{N}$. Therefore, in regard of

$$\sum_{\boldsymbol{\nu}' \le \boldsymbol{\nu}} \binom{\boldsymbol{\nu}}{\boldsymbol{\nu}'} |\boldsymbol{\nu}'|! |\boldsymbol{\nu} - \boldsymbol{\nu}'|! = (|\boldsymbol{\nu}| + 1)!,$$

see e.g. [33], we arrive at the assertion. ∎

Remark 6. The appearing factors of the form $c^{|\boldsymbol{\nu}|}$ in (2), $(2c)^{|\boldsymbol{\nu}|}$ in Theorem 4 and $\hat{c}^{|\boldsymbol{\nu}|}$ in Corollary 5 can always be removed by rescaling the sequences $\boldsymbol{\gamma}$ or $\widetilde{\boldsymbol{\gamma}}$ accordingly. Exemplarily, we obtain by exploiting $|\boldsymbol{\nu}| + 1 \le 2^{|\boldsymbol{\nu}|}$ and setting $\overline{\gamma}_k := 2\hat{c}\tilde{\gamma}_k$ that

$$\big\| \big[\partial_{\boldsymbol{y}}^{\boldsymbol{\nu}} \big[\phi\big(q(\boldsymbol{y})\big) \exp\big(-\Phi_\Gamma(\boldsymbol{y},\delta)\big)\big]\big] \big\|_{\mathcal{Z}} \le \hat{C} |\boldsymbol{\nu}|! \overline{\boldsymbol{\gamma}}^{\boldsymbol{\nu}} \quad \text{for all } \boldsymbol{\nu} \in \mathcal{F}_{\boldsymbol{\alpha}}.$$

Therefore, we may assume that all constants appearing in Theorem 4 and Corollary 5 are independent of the support size of $\boldsymbol{\nu} \in \mathcal{F}_{\boldsymbol{\alpha}}$.

3. Forward model.

3.1. The domain mapping method. In this section, we formulate the diffusion problem on random domains as is has been addressed in [33]. To that end, let $(\Omega, \mathcal{A}, \mathbb{P})$ denote a complete and separable probability space with σ-algebra $\mathcal{A}$ and probability measure $\mathbb{P}$. Here, complete means that $\mathcal{A}$ contains all $\mathbb{P}$-null sets. For a given Banach space $\mathcal{X}$, we introduce the Bochner space $L^p_{\mathbb{P}}(\Omega; \mathcal{X})$, $1 \le p \le \infty$, which consists of all equivalence classes of strongly measurable functions $v \colon \Omega \to \mathcal{X}$ whose norm

$$\|v\|_{L^p_{\mathbb{P}}(\Omega;\mathcal{X})} := \begin{cases} \left(\int_\Omega \|v(\cdot,\omega)\|_{\mathcal{X}}^p \, \mathrm{d}\mathbb{P}(\omega) \right)^{1/p}, & p < \infty \\ \operatorname*{ess\,sup}_{\omega \in \Omega} \|v(\cdot,\omega)\|_{\mathcal{X}}, & p = \infty \end{cases}$$

is finite. If $p = 2$ and $\mathcal{X}$ is a separable Hilbert space, then the Bochner space $L^p_{\mathbb{P}}(\Omega; \mathcal{X})$ is isomorphic to the tensor product space $L^2_{\mathbb{P}}(\Omega) \otimes \mathcal{X}$. For more details on Bochner spaces, we refer the reader to [36].

Now, given a random domain $D(\omega) \subset \mathbb{R}^d$ for $d = 2, 3$, we assume the existence of a reference domain $D_0 \subset \mathbb{R}^d$ and of a *uniform* C^1*-diffeomorphism* $\mathbf{V} \colon \overline{D_0} \times \Omega \to \mathbb{R}^d$, i.e.

$$\|\mathbf{V}(\omega)\|_{C^1(\overline{D_0};\mathbb{R}^d)}, \|\mathbf{V}^{-1}(\omega)\|_{C^1(\overline{D_0};\mathbb{R}^d)} \le C_{\mathrm{uni}} \quad \text{for } \mathbb{P}\text{-a.e. } \omega \in \Omega, \tag{10}$$

such that $D(\omega)$ is implicitly given by the relation

$$D(\omega) = \mathbf{V}(D_0, \omega).$$

Particularly, since $\mathbf{V} \in L^\infty\big(\Omega; C^1(\overline{D_0})\big) \subset L^2\big(\Omega; C^1(\overline{D_0})\big)$, the vector field $\mathbf{V}$ exhibits a Karhunen-Loève expansion of the form

$$\mathbf{V}(\mathbf{x}, \omega) = \mathbb{E}[\mathbf{V}](\mathbf{x}) + \sum_{k=1}^{\infty} \mathbf{V}_k(\mathbf{x}) Y_k(\omega). \tag{11}$$

The anisotropy which is induced by the spatial parts $\{\mathbf{V}_k\}_k$, describing the fluctuations around the nominal value $\mathbb{E}[\mathbf{V}](\mathbf{x})$, is encoded by

$$\gamma_k := \|\mathbf{V}_k\|_{W^{1,\infty}(D_0;\mathbb{R}^d)}. \tag{12}$$

For our modeling, we shall also make the following common assumptions.

Assumption 7.

(i) The random variables $\{Y_k\}_k$ take values in $[-1/2, 1/2]$.
(ii) The random variables $\{Y_k\}_k$ are independent and identically distributed.
(iii) The sequence $\{\gamma_k\}_k$ is at least in $\ell^1(\mathbb{N})$.

By an appropriate reparametrization, we can achieve that $\mathbb{E}[\mathbf{V}](\mathbf{x}) = \mathbf{x}$. Moreover, if we identify the random variables by their image $\boldsymbol{y} \in U = [-1/2, 1/2]^{\mathbb{N}}$, we end up with the representation

$$\mathbf{V}(\mathbf{x}, \boldsymbol{y}) = \mathbf{x} + \sum_{k=1}^{\infty} \mathbf{V}_k(\mathbf{x}) y_k. \tag{13}$$

The Jacobian of $\mathbf{V}$ with respect to the spatial variable $\mathbf{x}$ is thus given by

$$\mathbf{J}(\mathbf{x}, \boldsymbol{y}) = \mathbf{I} + \sum_{k=1}^{\infty} \mathbf{V}_k'(\mathbf{x}) y_k.$$

Introducing the parametric domains $D(\boldsymbol{y}) := \mathbf{V}(D_0, \boldsymbol{y})$, the forward problem which we consider here becomes:

Find $q \in H^1\big(D(\boldsymbol{y})\big)$ such that

$$\begin{aligned} -\Delta q(\boldsymbol{y}) &= 0 \quad \text{in } D(\boldsymbol{y}), \\ q(\boldsymbol{y}) &= g \quad \text{on } \partial D(\boldsymbol{y}). \end{aligned} \tag{14}$$

To guarantee the solvability of the model problem for every realization of the parameter $\boldsymbol{y} \in U$, it is reasonable to postulate that the Dirichlet data g are defined on the entire hold-all domain $\mathcal{D} := \cup_{\boldsymbol{y} \in U} D(\boldsymbol{y})$. Moreover, to derive regularity results that are independent of the parameter dimension, it is necessary that g is an analytic function, see [33]. Nevertheless, in view of (2), we shall weaken this estimate and only require that there holds

$$\|\partial_{\boldsymbol{y}}^{\boldsymbol{\nu}} (\Delta g \circ \mathbf{V})(\boldsymbol{y})\|_{L^\infty(D_0)} \leq C |\boldsymbol{\nu}|! c^{|\boldsymbol{\nu}|} \boldsymbol{\gamma}^{\boldsymbol{\nu}} \quad \text{for all } \boldsymbol{\nu} \in \mathcal{F}_{\boldsymbol{\alpha}} \tag{15}$$

for some constants $C, c > 0$. Thus, it would be sufficient to postulate $\Delta g \in C^{|\boldsymbol{\alpha}|}\big(D(\boldsymbol{y})\big)$ for all $\boldsymbol{y} \in U$. Hence, we can reformulate the problem by making the ansatz

$$q(\boldsymbol{y}) = q_0(\boldsymbol{y}) + g.$$

This results in:

Find $q_0 \in H_0^1\big(D(\boldsymbol{y})\big)$ such that

$$\begin{aligned} -\Delta q_0(\boldsymbol{y}) &= \Delta g \quad \text{in } D(\boldsymbol{y}), \\ q_0(\boldsymbol{y}) &= 0 \quad \text{on } \partial D(\boldsymbol{y}). \end{aligned}$$

From this, we can easily derive the variational formulation:

Find $q_0 \in H_0^1\big(D(\boldsymbol{y})\big)$ such that there holds for all $v \in H_0^1\big(D(\boldsymbol{y})\big)$ that

$$\int_{D(\boldsymbol{y})} \nabla q_0(\boldsymbol{y}) \nabla v \,\mathrm{d}\mathbf{x} = \int_{D(\boldsymbol{y})} (\Delta g) v \,\mathrm{d}\mathbf{x}.$$

Now, defining

$$\mathbf{A}(\mathbf{x}, \boldsymbol{y}) := \big[\mathbf{J}^\intercal \mathbf{J}\big]^{-1}(\mathbf{x}, \boldsymbol{y}) \det \mathbf{J}(\mathbf{x}, \boldsymbol{y}) \quad \text{and} \quad \hat{f}(\mathbf{x}, \boldsymbol{y}) := (\Delta g)\big(\mathbf{V}(\mathbf{x}, \boldsymbol{y})\big) \det \mathbf{J}(\mathbf{x}, \boldsymbol{y}), \tag{16}$$

we arrive at the variational formulation on the reference domain D_0, which reads:

Find $\hat{q}_0 \in H_0^1(D_0)$ such that there holds for all $v \in H_0^1(D_0)$ that

$$\int_{D_0} \mathbf{A}(\boldsymbol{y}) \nabla \hat{q}_0(\boldsymbol{y}) \nabla v \,\mathrm{d}\mathbf{x} = \int_{D_0} \hat{f}(\boldsymbol{y}) v \,\mathrm{d}\mathbf{x}.$$

We note that $q_0(\boldsymbol{y}) = \hat{q}_0 \circ \mathbf{V}^{-1}(\boldsymbol{y})$ and for all $\boldsymbol{y} \in U$, we derive

$$\big\|\partial_{\boldsymbol{y}}^{\boldsymbol{\nu}} \hat{q}_0(\boldsymbol{y})\big\|_{H_0^1(D_0)} \leq C|\boldsymbol{\nu}|! c^{|\boldsymbol{\nu}|} \boldsymbol{\gamma}^{\boldsymbol{\nu}} \quad \text{for all } \boldsymbol{\nu} \in \mathcal{F}_{\boldsymbol{\alpha}}, \tag{17}$$

for a sequence $\boldsymbol{\gamma} \in \ell^p(\mathbb{N})$ for some $p < 1$, given here by (12), and some constants $C, c > 0$, see [33] for the details. A regularity estimate similar to (17) particularly accounts for the system response $\hat{q}$ of the forward problem (14) transported to D_0, which is a straightforward consequence of the smoothness requirements (15) in the Dirichlet data and the application of the Faà di Bruno's formula.

3.2. Dimension truncation. In this subsection, we shall supplement the analysis presented in [33] by discussing the error of dimension truncation. As a starting point, we consider the general representation (13) of the vector field. We refer to s as the *truncation dimension* or *parametric dimension* of the problem. By considering now sequences of the form $\boldsymbol{y} = \{y_1, \ldots, y_s, 0, \ldots\}$, the following lemma is immediate.

Lemma 8. *Let the Jacobian of the truncated expansion of the vector field* $\mathbf{V}$ *be defined as*

$$\mathbf{J}^{(s)}(\mathbf{x}, \boldsymbol{y}) := \mathbf{I} + \sum_{k=1}^{s} \mathbf{V}_k'(\mathbf{x}) y_k \quad \textit{and set} \quad \varepsilon_{\boldsymbol{\gamma}}^{(s)} := \sum_{k=s+1}^{\infty} \gamma_k.$$

Then, there holds

$$\frac{1}{C_{\mathrm{uni}}} \leq \big\|\mathbf{J}^{(s)}(\boldsymbol{y})\big\|_{L^\infty(D_0; \mathbb{R}^{d \times d})} \leq C_{\mathrm{uni}}$$

with the same constant as in (10)*, where the bounds hold uniformly in* s*.*

Now, we consider the impact of truncation on $\det \mathbf{J}(\boldsymbol{y})$ and $\big[\mathbf{J}^\intercal\mathbf{J}\big](\boldsymbol{y})$ separately.

Lemma 9. *The determinant of the truncated Jacobian satisfies the estimate*

$$\big|\det \mathbf{J}(\boldsymbol{y}) - \det \mathbf{J}^{(s)}(\boldsymbol{y})\big| \leq dC_{\mathrm{uni}}^{d-1}\varepsilon_{\boldsymbol{\gamma}}^{(s)}.$$

Proof. For the determinant function and two matrices $\mathbf{M}, \mathbf{M}' \in \mathbb{R}^{d\times d}$ with bounded columns $\|\mathbf{M}_i\|_2, \|\mathbf{M}_i'\|_2 \leq c$ for $i = 1, \dots, d$ and $c > 0$, we know

$$|\det \mathbf{M} - \det \mathbf{M}'| \leq dc^{d-1}\|\mathbf{M} - \mathbf{M}'\|_2.$$

Obviously, we can bound each column of $\mathbf{J}$ and $\mathbf{J}^{(s)}$ by C_{uni}. Therefore, we arrive at

$$\big|\det \mathbf{J}(\boldsymbol{y}) - \det \mathbf{J}^{(s)}(\boldsymbol{y})\big| \leq dC_{\mathrm{uni}}^{d-1}\big\|\mathbf{J}(\boldsymbol{y}) - \mathbf{J}^{(s)}(\boldsymbol{y})\big\|_2 \leq dC_{\mathrm{uni}}^{d-1}\varepsilon_{\boldsymbol{\gamma}}^{(s)}.$$ ∎

Lemma 10. *For the truncation of the matrix $\big[\mathbf{J}^\intercal\mathbf{J}\big]^{-1}(\boldsymbol{y})$, there holds the estimate*

$$\big\|\big[\mathbf{J}^\intercal\mathbf{J}\big]^{-1}(\boldsymbol{y}) - \big[\big(\mathbf{J}^{(s)}\big)^\intercal\mathbf{J}^{(s)}\big]^{-1}(\boldsymbol{y})\big\|_{L^\infty(D_0;\mathbb{R}^{d\times d})} \leq \frac{2}{C_{\mathrm{uni}}^3}\varepsilon_{\boldsymbol{\gamma}}^{(s)} + O\big(\varepsilon_{\boldsymbol{\gamma}}^{(s)}\big)^2.$$

Proof. A straightforward calculation yields

$$\big\|[\mathbf{J}^\intercal\mathbf{J}](\boldsymbol{y}) - \big[\big(\mathbf{J}^{(s)}\big)^\intercal\mathbf{J}^{(s)}\big](\boldsymbol{y})\big\|_{L^\infty(D_0;\mathbb{R}^{d\times d})} \leq 2C_{\mathrm{uni}}\varepsilon_{\boldsymbol{\gamma}}^{(s)} + O\big(\varepsilon_{\boldsymbol{\gamma}}^{(s)}\big)^2.$$

Moreover, for two Matrices $\mathbf{M}, \mathbf{M}' \in \mathbb{R}^{d\times d}$, a first order Taylor expansion yields

$$\mathbf{M}^{-1} = (\mathbf{M}')^{-1} - (\mathbf{M}')^{-1}(\mathbf{M} - \mathbf{M}')(\mathbf{M}')^{-1} + O\big((\mathbf{M} - \mathbf{M}')^2\big).$$

The latter can easily be verified using the first and second order Gâteaux derivatives of the Function $f(\mathbf{M}) = \mathbf{M}^{-1}$ at the point $\mathbf{M}'$ with respect to the direction $\mathbf{D} = \mathbf{M} - \mathbf{M}'$.

Therefore, we conclude

$$\begin{aligned}
&\big\|\big[\mathbf{J}^\intercal\mathbf{J}\big]^{-1}(\boldsymbol{y}) - \big[\big(\mathbf{J}^{(s)}\big)^\intercal\mathbf{J}^{(s)}\big]^{-1}(\boldsymbol{y})\big\|_{L^\infty(D_0;\mathbb{R}^{d\times d})} \\
&\quad\leq 2C_{\mathrm{uni}}\varepsilon_{\boldsymbol{\gamma}}^{(s)}\big\|\big[\mathbf{J}^\intercal\mathbf{J}\big]^{-1}(\boldsymbol{y})\big\|_{L^\infty(D_0;\mathbb{R}^{d\times d})}^2 + O\big(\varepsilon_{\boldsymbol{\gamma}}^{(s)}\big)^2 \\
&\quad\leq 2\frac{C_{\mathrm{uni}}}{C_{\mathrm{uni}}^4}\varepsilon_{\boldsymbol{\gamma}}^{(s)} + O\big(\varepsilon_{\boldsymbol{\gamma}}^{(s)}\big)^2,
\end{aligned}$$

where we applied the bound

$$\big\|\big[\mathbf{J}^\intercal\mathbf{J}\big]^{-1}(\boldsymbol{y})\big\|_{L^\infty(D_0;\mathbb{R}^{d\times d})} \leq \frac{1}{C_{\mathrm{uni}}^2}.$$ ∎

Having these lemmata at hand, we can bound the truncation error in the diffusion matrix and in the right hand side.

Theorem 11. *The truncation errors in the diffusion matrix and in the right hand side satisfy the error estimates*

$$\left\|\mathbf{A}(\boldsymbol{y}) - \mathbf{A}^{(s)}(\boldsymbol{y})\right\|_{L^\infty(D_0;\mathbb{R}^{d\times d})} \leq (2+d)C_{\mathrm{uni}}^{d-3}\varepsilon_{\boldsymbol{\gamma}}^{(s)} + O\big(\varepsilon_{\boldsymbol{\gamma}}^{(s)}\big)^2$$

and

$$\left\|\hat{f}(\boldsymbol{y}) - \hat{f}^{(s)}(\boldsymbol{y})\right\|_{L^\infty(D_0)} \leq (d + C_{\mathrm{uni}})\|\Delta g\|_{W^{1,\infty}} C_{\mathrm{uni}}^{d-1}\varepsilon_{\boldsymbol{\gamma}}^{(s)}.$$

In these estimates, the quantities $\mathbf{A}^{(s)}(\boldsymbol{y})$ and $\hat{f}^{(s)}(\boldsymbol{y})$ are simply obtained by replacing $\mathbf{J}$ in (16) by $\mathbf{J}^{(s)}$.

Proof. By the application of the triangle inequality, we can now simply bound the truncation error for the diffusion matrix according to

$$\begin{aligned}
&\left\|\mathbf{A}(\boldsymbol{y}) - \mathbf{A}^{(s)}(\boldsymbol{y})\right\|_{L^\infty(D_0;\mathbb{R}^{d\times d})} \\
&\quad\leq \left\|\mathbf{A}(\boldsymbol{y}) - \left[\mathbf{J}^\intercal\mathbf{J}\right]^{-1}(\boldsymbol{y})\det\mathbf{J}^{(s)}(\boldsymbol{y})\right\|_{L^\infty(D_0;\mathbb{R}^{d\times d})} \\
&\qquad + \left\|\left[\mathbf{J}^\intercal\mathbf{J}\right]^{-1}(\boldsymbol{y})\det\mathbf{J}^{(s)}(\boldsymbol{y}) - \mathbf{A}^{(s)}(\boldsymbol{y})\right\|_{L^\infty(D_0;\mathbb{R}^{d\times d})} \\
&\quad\leq \frac{1}{C_{\mathrm{uni}}^2} d C_{\mathrm{uni}}^{d-1}\varepsilon_{\boldsymbol{\gamma}}^{(s)} + \frac{2}{C_{\mathrm{uni}}^3}\varepsilon_{\boldsymbol{\gamma}}^{(s)} C_{\mathrm{uni}}^{d} + O\big(\varepsilon_{\boldsymbol{\gamma}}^{(s)}\big)^2 \\
&\quad\leq (2+d)C_{\mathrm{uni}}^{d-3}\varepsilon_{\boldsymbol{\gamma}}^{(s)} + O\big(\varepsilon_{\boldsymbol{\gamma}}^{(s)}\big)^2.
\end{aligned}$$

where we applied the bounds

$$\left\|\left[\mathbf{J}^\intercal\mathbf{J}\right]^{-1}(\boldsymbol{y})\right\|_{L^\infty(D_0;\mathbb{R}^{d\times d})} \leq \frac{1}{C_{\mathrm{uni}}^2} \quad \text{and} \quad \left|\det\mathbf{J}^{(s)}(\boldsymbol{y})\right| \leq C_{\mathrm{uni}}^d.$$

In complete analogy, we can bound the truncation error in the right hand side according to

$$\begin{aligned}
&\left\|\hat{f}(\boldsymbol{y}) - \hat{f}^{(s)}(\boldsymbol{y})\right\|_{L^\infty(D_0)} \\
&\quad\leq \left\|\hat{f}(\boldsymbol{y}) - (\Delta g\circ\mathbf{V})(\boldsymbol{y})\det\mathbf{J}^{(s)}(\boldsymbol{y})\right\|_{L^\infty(D_0)} \\
&\qquad + \left\|(\Delta g\circ\mathbf{V})(\boldsymbol{y})\det\mathbf{J}^{(s)}(\boldsymbol{y}) - \hat{f}^{(s)}(\boldsymbol{y})\right\|_{L^\infty(D_0)} \\
&\quad\leq \|\Delta g\|_{L^\infty(D)} d C_{\mathrm{uni}}^{d-1}\varepsilon_{\boldsymbol{\gamma}}^{(s)} + \|\Delta g\|_{W^{1,\infty}(D)}\varepsilon_{\boldsymbol{\gamma}}^{(s)} C_{\mathrm{uni}}^{d} \\
&\quad\leq (d + C_{\mathrm{uni}})\|\Delta g\|_{W^{1,\infty}} C_{\mathrm{uni}}^{d-1}\varepsilon_{\boldsymbol{\gamma}}^{(s)}.
\end{aligned}$$

■

From Lemma 8, we infer that the diffusion matrix $\mathbf{A}^{(s)}(\boldsymbol{y})$ is always elliptic, i.e. there holds

$$\mathbf{z}^\intercal\mathbf{A}^{(s)}(\mathbf{x},\boldsymbol{y})\mathbf{z} \geq a_{\min} > 0 \quad \text{for all } \mathbf{z}\in\mathbb{R}^d \text{ uniformly in } s.$$

Thus, let $\hat{q}_0^{(s)} \in H_0^1(D_0)$ be the unique solution of the variational formulation

$$\int_{D_0} \mathbf{A}^{(s)}(\boldsymbol{y})\nabla\hat{q}_0^{(s)}\nabla v\,\mathrm{d}\mathbf{x} = \int_{D_0}\hat{f}^{(s)}(\boldsymbol{y})v\,\mathrm{d}\mathbf{x}.$$

Having the impact of truncating the Jacobian on the diffusion coefficient and the right hand side at hand, we may now bound the respective error of the solution in analogy to Strang's lemma.

Theorem 12. *There holds for a constant $C > 0$, which depends on the domain D_0, the spatial dimension d as well as $\|\Delta g\|_{W^{1,\infty}}$ and C_{uni}, the error estimate*

$$\big\|\big(\hat{q}_0 - \hat{q}_0^{(s)}\big)(\boldsymbol{y})\big\|_{H_0^1(D_0)} \leq \frac{C}{a_{\min}}\big(1 + \|\hat{q}_0(\boldsymbol{y})\|_{H_0^1(D_0)}\big)\varepsilon_{\boldsymbol{\gamma}}^{(s)} + O\big(\varepsilon_{\boldsymbol{\gamma}}^{(s)}\big)^2.$$

Proof. Making use of the ellipticity of the bilinear form induced by $\mathbf{A}^{(s)}(\boldsymbol{y})$, we have

$$\begin{aligned}
&a_{\min}\big\|\big(\hat{q}_0 - \hat{q}_0^{(s)}\big)(\boldsymbol{y})\big\|_{H_0^1(D_0)}^2 \\
&\quad\leq \int_{D_0} \mathbf{A}^{(s)}(\boldsymbol{y})\nabla\big(\hat{q}_0 - \hat{q}_0^{(s)}\big)(\boldsymbol{y})\nabla\big(\hat{q}_0 - \hat{q}_0^{(s)}\big)(\boldsymbol{y})\,\mathrm{d}\mathbf{x} \\
&\quad= \int_{D_0} \mathbf{A}^{(s)}(\boldsymbol{y})\nabla\hat{q}_0(\boldsymbol{y})\nabla\big(\hat{q}_0 - \hat{q}_0^{(s)}\big)(\boldsymbol{y})\,\mathrm{d}\mathbf{x} - \int_{D_0} \hat{f}^{(s)}(\boldsymbol{y})\big(\hat{q}_0 - \hat{q}_0^{(s)}\big)(\boldsymbol{y})\,\mathrm{d}\mathbf{x} \\
&\quad= \int_{D_0} \big(\mathbf{A}^{(s)} - \mathbf{A}\big)(\boldsymbol{y})\nabla\hat{q}_0(\boldsymbol{y})\nabla\big(\hat{q}_0 - \hat{q}_0^{(s)}\big)(\boldsymbol{y})\,\mathrm{d}\mathbf{x} \\
&\qquad- \int_{D_0} \big(\hat{f}^{(s)} - \hat{f}\big)(\boldsymbol{y})\big(\hat{q}_0 - \hat{q}_0^{(s)}\big)(\boldsymbol{y})\,\mathrm{d}\mathbf{x} \\
&\quad\leq \big\|\mathbf{A}(\boldsymbol{y}) - \mathbf{A}^{(s)}(\boldsymbol{y})\big\|_{L^\infty(D_0;\mathbb{R}^{d\times d})}\big\|\big(\hat{q}_0 - \hat{q}_0^{(s)}\big)(\boldsymbol{y})\big\|_{H_0^1(D_0)}\|\hat{q}_0(\boldsymbol{y})\|_{H_0^1(D_0)} \\
&\qquad+ \big\|\hat{f}(\boldsymbol{y}) - \hat{f}^{(s)}(\boldsymbol{y})\big\|_{H^{-1}(D_0)}\big\|\big(\hat{q}_0 - \hat{q}_0^{(s)}\big)(\boldsymbol{y})\big\|_{H_0^1(D_0)}.
\end{aligned}$$

Now, we exploit

$$\big\|\hat{f}(\mathbf{y}) - \hat{f}^{(s)}(\mathbf{y})\big\|_{H^{-1}(D_0)} \leq c_P\sqrt{|D_0|}\big\|\hat{f}(\mathbf{y}) - \hat{f}^{(s)}(\mathbf{y})\big\|_{L^\infty(D_0)},$$

where $c_P > 0$ is the Poincare constant for D_0 and $|D_0|$ is the Lebesgue measure of D_0. Then, simplifying this expression and inserting the bounds from Theorem 11 results in

$$\begin{aligned}
\big\|\big(\hat{q}_0 - \hat{q}_0^{(s)}\big)(\boldsymbol{y})\big\|_{H_0^1(D_0)} \leq{}& \frac{1}{a_{\min}}(2+d)C_{\mathrm{uni}}^{d-3}\varepsilon_{\boldsymbol{\gamma}}^{(s)}\|\hat{q}_0(\boldsymbol{y})\|_{H_0^1(D_0)} + O\big(\varepsilon_{\boldsymbol{\gamma}}^{(s)}\big)^2 \\
&+ \frac{1}{a_{\min}}c_P\sqrt{|D_0|}(d + C_{\mathrm{uni}})\|\Delta g\|_{W^{1,\infty}}C_{\mathrm{uni}}^{d-1}\varepsilon_{\boldsymbol{\gamma}}^{(s)}.
\end{aligned}$$

∎

Remark 13. Taking the previous theorem as a starting point, it is easy to derive

$$\big\|\big(\phi(\hat{q}_0) - \phi(\hat{q}_0^{(s)})\big)(\boldsymbol{y})\big\|_{\mathcal{Z}} \leq C\varepsilon_{\boldsymbol{\gamma}}^{(s)}$$

for some constant $C > 0$, given that the quantity of interest $\phi\colon H_0^1(D_0) \to \mathcal{Z}$ is at least Lipschitz continuous.

The preceeding analysis establishes an estimate of the dimension truncation error for the system response, pointwise in $\boldsymbol{y}$, depending on the remainder $\varepsilon_{\boldsymbol{\gamma}}^{(s)}$. Next, we reformulate this in terms of the p-summability of the sequence $\boldsymbol{\gamma}$.

Lemma 14. *Let $\varepsilon_{\boldsymbol{\gamma}}^{(s)}$ be defined as in Lemma 8. Assume that the sequence $\boldsymbol{\gamma}$ is nonincreasing, $\gamma_1 \geq \gamma_2 \ldots$, and assume additionally that there exists $p \in (0,1)$ such that $\boldsymbol{\gamma} \in \ell^p(\mathbb{N})$. Then,*

$$\varepsilon_{\boldsymbol{\gamma}}^{(s)} \leq C(p,\boldsymbol{\gamma}) s^{-1/p+1}, \tag{18}$$

with $C(p,\boldsymbol{\gamma}) = \min\left((1/p-1)^{-1},1\right)\|\boldsymbol{\gamma}\|_{\ell^p}$.

Proof. See e.g. [17, Thm. 2.6]. ∎

The bound in Remark 13 applies to the pointwise dimension truncation error, i.e. for a fixed $\boldsymbol{y} \in U$. However, we aim to approximate expectations over $\boldsymbol{y}$; in this case, in which the variables y_j are integrated out, higher dimension truncation convergence rates can be obtained. The following statement is required for the analysis of the total error in Section 5.2 and concerns the dimension truncation error of the integral, with respect to the parameter sequence $\boldsymbol{y}$, of a functional of the system response, as this is what is computed both in forward and Bayesian inverse UQ.

Lemma 15. *Let $\phi\colon H_0^1(D_0) \to \mathcal{Z}$ denote a quantity of interest functional that is at least Lipschitz continuous. Then, there exists a $C > 0$ depending on p and $\boldsymbol{\gamma}$ such that*

$$\left\| \int_U \left(\phi(q(\boldsymbol{y})) - \phi(q^{(s)}(\boldsymbol{y}))\right) \mu(\mathrm{d}\boldsymbol{y}) \right\|_{\mathcal{Z}} \leq C s^{-\theta/p+1}, \tag{19}$$

where $\theta = 1$ in general for μ being either the prior or posterior measure. In the case that $q(\boldsymbol{y})$ is the solution to an affine-parametric operator equation and the measure μ is centered with bounded moments we have $\theta = 2$.

Proof. Exploiting the Lipschitz dependence of the solution $q(\boldsymbol{y})$ on the parametrization from (13), we can proceed as in [18, Thm. 2.1] and [42]. The case of a posterior distribution is considered in [16] and the affine-parametric case is considered in detail in [24]. ∎

Remark 16. Note that the coefficient obtained by the domain mapping method involves a nonlinear function of the boundary parametrization, implying $\theta = 1$ in Lemma 15. However, it was observed in [23] that $\theta = 2$ seems to hold in various non-affine cases, in particular for Bayesian inversion and for a similar example in domain uncertainty.

4. Electrical Impedance Tomography. Now, let $\mathcal{D} \subset \mathbb{R}^2$ denote a simply-connected and convex domain with Lipschitz continuous boundary $\Sigma := \partial\mathcal{D}$. Inside the domain, we suppose that there exists a simply connected subdomain $S \Subset \mathcal{D}$ with boundary $\Gamma := \partial S$. The boundary Γ shall be of co-dimension 1 and, thus, separate the interior domain S and the outer domain $\mathcal{D}$. The resulting, annular domain $\mathcal{D} \setminus \overline{S}$ shall be referred to as D.

A sketch of the situation can be found in Figure 1. The inner domain S models a material of constant conductivity that is significantly different from the (also constant) conductivity of the material in the annular domain D. We are interested in the identification of the inclusion S. To that end, for a given voltage distribution $g_{\mathrm{D}} \in H^{1/2}(\Sigma)$, we measure the corresponding current distribution $g_{\mathrm{N}} \in H^{-1/2}(\Sigma)$. This means that we are looking for a domain D which

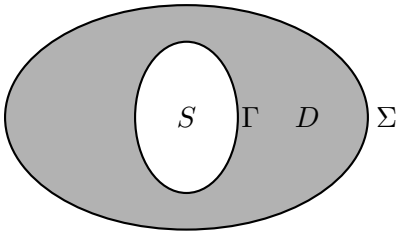

Figure 1: The domain D with inner and outer boundaries Γ and Σ, respectively, and the inclusion S.

satisfies the overdetermined boundary value problem

$$\begin{aligned} \Delta q &= 0 && \text{in } D, \\ \gamma_{0,\Gamma}^{\text{int}} q &= 0 && \text{on } \Gamma, \\ \gamma_{0,\Sigma}^{\text{int}} q &= g_{\text{D}} && \text{on } \Sigma, \\ \gamma_{1,\Sigma}^{\text{int}} q &= g_{\text{N}} && \text{on } \Sigma. \end{aligned} \tag{20}$$

Herein, the operators $\gamma_{0,\Gamma}^{\text{int}}$ and $\gamma_{0,\Sigma}^{\text{int}}$ denote the interior trace operators at Γ and Σ, respectively, whereas $\gamma_{1,\Sigma}^{\text{int}}$ is the co-normal derivative at Σ. Instead of successively solving this problem by an optimization procedure, as it has been done in e.g. [20], we will approach it here by means of Bayesian inversion. In this context, we assume that the measured Neumann data at Σ are subject to uncertainty and assume a prior distribution on the parameters describing the boundary. In order to quantify the resulting uncertainty inherent in this problem, we reformulate the associated forward problem in terms of an elliptic diffusion problem which is stated on a random domain.

Due to our lack of knowledge on the shape of the inclusion, we consider the interior domain to be random. This uncertainty is incorporated by assuming the interior boundary to be $\mathbb{P}$-a.s. star-shaped and modeling it according to

$$\Gamma(\omega) = \big\{ \mathbf{x} = \boldsymbol{\sigma}(t,\omega) \in \mathbb{R}^2 : \boldsymbol{\sigma}(t,\omega) = u(t,\omega)\mathbf{e}(t),\ t \in I \big\}, \tag{21}$$

where $\boldsymbol{\sigma}(t,\omega)$ is a random field. Furthermore, let $\mathbf{e}(t) := [\cos(t), \sin(t)]^\intercal$ denote the radial direction and $I := [0, 2\pi]$ be the interval for the angle t. We note that with the techniques presented in the previous section it is possible to treat more general inclusions. Nevertheless, our particular choice facilitates a sensible definition of an expected shape. Additionally, the variance (or higher moments) of the parameters can be computed, yielding via (21) a confidence region for the inclusion. In accordance with [31], we define the boundary's mean and variance as

$$\begin{aligned} \mathbb{E}[\Gamma(\omega)] &= \big\{ \mathbf{x} \in \mathbb{R}^2 : \mathbf{x} = \mathbb{E}[u(t,\omega)]\mathbf{e}(t),\ t \in I \big\} \\ \mathbb{V}[\Gamma(\omega)] &= \big\{ \mathbf{x} \in \mathbb{R}^2 : \mathbf{x} = \mathbb{V}[u(t,\omega)]\mathbf{e}(t),\ t \in I \big\}. \end{aligned}$$

To that end, the radial function $u(t,\omega) \geq \underline{c} > 0$ has to be in the Bochner space $L^2\big(\Omega; C^2_{\mathrm{per}}(I)\big)$, where $C^2_{\mathrm{per}}(I)$ denotes the Banach space of periodic, twice continuously differentiable functions, i.e.

$$C^2_{\mathrm{per}}(I) := \big\{ f \in C^2(I) : f^{(i)}(0) = f^{(i)}(2\pi),\ i = 0,1,2 \big\},$$

equipped with the norm

$$\|f\|_{C^2_{\mathrm{per}}(I)} := \sum_{i=0}^{2} \max_{x \in I} \big| f^{(i)}(x) \big|.$$

If $u(t,\omega)$ is described by its expectation

$$\mathbb{E}[u](t) = \int_\Omega u(t,\omega)\, \mathrm{d}\mathbb{P}(\omega)$$

and its covariance

$$\mathrm{Cov}[u](t,t') = \mathbb{E}[u(t,\omega)u(t,\omega)] = \int_\Omega u(t,\omega)u(t',\omega)\, \mathrm{d}\mathbb{P}(\omega),$$

then we can represent it by its *Karhunen-Loève expansion*, cf. [43],

$$u(t,\omega) = \mathbb{E}[u](t) + \sum_{k=1}^{\infty} u_k(t) Y_k(\omega).$$

Herein, the functions $\{u_k(\varphi)\}_k$ are scaled versions of the eigenfunctions of the Hilbert-Schmidt operator associated to $\mathrm{Cov}[u](t,t')$. Common approaches to numerically recover the Karhunen-Loève expansion from these quantities are e.g. given in [32, 50]. We would like to emphasize that the chosen representation of the random vector field (13) in terms of polar coordinates is only one possibility, given a star shaped inclusion. Alternative and more flexible approaches would describe the spatial functions $\mathbf{V}_k$ by e.g. B-splines [37, 46] or other systems with finite support [25, 26]. See particularly [19], wherein star-shaped inclusions are considered, along with two additional approaches: an unknown coefficient function and a so-called level-set prior.

By construction, the random variables $\{Y_k(\omega)\}_k$ in the Karhunen-Loève expansion are uncorrelated. For our modeling, we shall also impose the conditions of Assumption 7, where we modify the third condition as follows:

(iii)' The sequence $\{\hat{\gamma}_k\}_k := \big\{ \|u_k\|_{W^{1,\infty}(0,2\pi)} \big\}_k$ is at least in $\ell^1(\mathbb{N})$.

The domain $D(\omega)$ shall now be identified by its boundaries $\Gamma(\omega)$ and Σ. Then, we face the following forward problem:

Find $q \in H^1\big(D(\omega)\big)$ such that

$$\begin{aligned} -\Delta q(\omega) &= 0 \quad && \text{in } D(\omega), \\ q(\omega) &= g \quad && \text{on } \partial D(\omega), \end{aligned} \tag{22}$$

where $g|_{\Gamma(\omega)} = 0$ and $g|_\Sigma = g_{\mathrm{D}}$.

The parametric regularity may now be obtained as in the previous section. To that end, we cast the forward model into the framework of the domain mapping method as it has been

done in [33] and employ the regularity results presented there. The boundary $\Gamma(\omega)$ in (21) is already parametrized with respect to the reference boundary $\Gamma_0 := \mathbb{E}[\Gamma]$. Hence, it is sensible to introduce the reference domain $D_0 \subset \mathbb{R}^2$ that is enclosed by the boundaries Γ_0 and Σ.

Thus, by a suitable extension, we can achieve that $\Gamma(\omega)$ is given by the application of a vector field $\mathbf{V}\colon \overline{D_0} \times \Omega \to \mathbb{R}^2$, i.e. $\Gamma(\omega) = \mathbf{V}(\Gamma_0, \omega)$. If Γ_0 is of class C^2, a possibility to define $\mathbf{V}$ is given as follows:

$$\mathbf{V}(\mathbf{x}, \omega) := \mathbf{x} + \sum_{k=1}^{\infty} u_k(\arg P\mathbf{x}) \begin{bmatrix} \cos(\arg P\mathbf{x}) \\ \sin(\arg P\mathbf{x}) \end{bmatrix} B(\|\mathbf{x} - P\mathbf{x}\|_2) Y_k(\omega), \tag{23}$$

where $P\mathbf{x}$ is the orthogonal projection of $\mathbf{x}$ onto Γ_0 and $B\colon [0,\infty) \to [0,1]$ is a smooth blending function with $B(0) = 1$ and $B(t) = 0$ for all $t \geq \operatorname{ess\,inf}_{\omega\in\Omega} \operatorname{dist}\big(\Gamma(\omega), \Sigma\big)$. Notice that if Γ_0 is of class C^2, the orthogonal projection P onto Γ_0 and thus $\mathbf{V}(\mathbf{x}, \omega)$ is at least of class C^1, cf. [40]. By this choice of B, we particularly guarantee that $\mathbf{V}(\Sigma, \omega) = \Sigma$. Finally, after a possible scaling of the perturbation's amplitude, we can always guarantee that this choice of $\mathbf{V}$ satisfies the uniformity condition (10), cp. [51]. Now, assuming that

$$\gamma_k := \left\| u_k \begin{bmatrix} \cos(\arg P\cdot) \\ \sin(\arg P\cdot) \end{bmatrix} B(\|\cdot - P\cdot\|_2) \right\|_{W^{1,\infty}(D_0,\mathbb{R}^2)}$$

is still in $\ell^1(\mathbb{N})$, we can carry over the regularity results from the previous section to our forward model (22) one-to-one.

Remark 17. Since we aim at reconstructing the inclusion S from measurements of the Neumann data at the fixed boundary Σ and since we impose that $\mathbf{V}(\Sigma, \omega) = \Sigma$, the Cauchy data, i.e. Dirichlet data and Neumann data, are independent of the particular choice of the blending function.

4.1. Discretization. Our approach to determine for the given pair $[\gamma_{0,\Sigma}^{\mathrm{int}} q, \gamma_{0,\Gamma(\boldsymbol{y})}^{\mathrm{int}} q] = [g_{\mathrm{D}}, 0]$ the respective solution $q(\mathbf{x}, \boldsymbol{y})$ to (14) relies on the reformulation of the boundary value problem as a boundary integral equation by means of Green's fundamental solution

$$k(\mathbf{x}, \mathbf{x}') = -\frac{1}{2\pi} \log \|\mathbf{x} - \mathbf{x}'\|_2.$$

Namely, the solution $q(\mathbf{x}, \boldsymbol{y})$ of (20) is given in each point $\mathbf{x} \in D(\boldsymbol{y})$ by Green's representation formula

$$q(\mathbf{x}, \boldsymbol{y}) = \int_{\Gamma(\boldsymbol{y})\cup\Sigma} k(\mathbf{x}, \mathbf{x}') \gamma_1^{\mathrm{int}} q(\mathbf{x}', \boldsymbol{y}) - \frac{\partial k(\mathbf{x}, \mathbf{x}')}{\partial \mathbf{n}_{\mathbf{x}'}} \gamma_0^{\mathrm{int}} q(\mathbf{x}', \boldsymbol{y}) \, \mathrm{d}s_{\mathbf{x}'}. \tag{24}$$

Using the jump properties of the layer potentials, we arrive at the direct boundary integral formulation which reads

$$\frac{1}{2} \gamma_0^{\mathrm{int}} q(\mathbf{x}, \boldsymbol{y}) = \int_{\Gamma(\boldsymbol{y})\cup\Sigma} k(\mathbf{x}, \mathbf{x}') \gamma_1^{\mathrm{int}} q(\mathbf{x}', \boldsymbol{y}) \, \mathrm{d}s_{\mathbf{x}'} - \int_{\Gamma(\boldsymbol{y})\cup\Sigma} \frac{\partial k(\mathbf{x}, \mathbf{x}')}{\partial \mathbf{n}_{\mathbf{x}'}} \gamma_0^{\mathrm{int}} q(\mathbf{x}', \boldsymbol{y}) \, \mathrm{d}s_{\mathbf{x}'}, \tag{25}$$

where $\mathbf{x} \in \Gamma(\boldsymbol{y}) \cup \Sigma$, see e.g. [47]. If we label the boundaries by $A, B \in \{\Gamma(\boldsymbol{y}), \Sigma\}$, then (25) includes the single layer operator

$$\mathcal{V} : C(A) \to C(B), \quad \big(\mathcal{V}_{AB}\rho\big)(\mathbf{x}) = -\frac{1}{2\pi} \int_A \log \|\mathbf{x} - \mathbf{x}'\|_2 \, \rho(\mathbf{x}') \, \mathrm{d}s_{\mathbf{x}'}, \tag{26}$$

and the double layer operator

$$\mathcal{K} : C(A) \to C(B), \quad \big(\mathcal{K}_{AB}\rho\big)(\mathbf{x}) = \frac{1}{2\pi} \int_A \frac{\langle \mathbf{x} - \mathbf{x}', \mathbf{n}_{\mathbf{x}'} \rangle}{\|\mathbf{x} - \mathbf{x}'\|_2^2} \rho(\mathbf{x}') \, \mathrm{d}s_{\mathbf{x}'}, \tag{27}$$

with the densities $\rho \in C(A)$ being the Cauchy data of q on A. The equation (25) in combination with (26) and (27) indicates the Dirichlet-to-Neumann map, which for problem (14) induces the following system of integral equations

$$\begin{bmatrix} \mathcal{V}_{\Sigma\Sigma} & \mathcal{V}_{\Sigma\Gamma(\boldsymbol{y})} \\ \mathcal{V}_{\Gamma(\boldsymbol{y})\Sigma} & \mathcal{V}_{\Gamma(\boldsymbol{y})\Gamma(\boldsymbol{y})} \end{bmatrix} \begin{bmatrix} \rho_\Sigma \\ \rho_{\Gamma(\boldsymbol{y})} \end{bmatrix} = \begin{bmatrix} 1/2\,\mathrm{Id} + \mathcal{K}_{\Sigma\Sigma} & \mathcal{K}_{\Sigma\Gamma(\boldsymbol{y})} \\ \mathcal{K}_{\Gamma(\boldsymbol{y})\Sigma} & 1/2\,\mathrm{Id} + \mathcal{K}_{\Gamma(\boldsymbol{y})\Gamma(\boldsymbol{y})} \end{bmatrix} \begin{bmatrix} g_\mathrm{D} \\ 0 \end{bmatrix}, \tag{28}$$

where Id denotes the identity operator. The boundary integral operator on the left hand side of this coupled system of boundary integral equations is uniformly elliptic and continuous provided that $\operatorname{diam}\big(D(\boldsymbol{y})\big) = \operatorname{diam}(\Sigma) < 1$. This guarantees the unique solvability by the Lax-Milgram lemma, see e.g. [52].

For the approximation of the unknown Cauchy data, we use the collocation method based on trigonometric polynomials. Applying the trapezoidal rule for the numerical quadrature and the regularization technique along the lines of [41] to deal with the singular integrals, we arrive at an exponentially convergent Nyström method provided that the data and the boundaries and thus the solution are analytic. More precisely, we have the following result.

Proposition 18. *Let $\rho \in C^k\big(\partial D(\boldsymbol{y})\big)$ be the solution to (28). Then, there holds*

$$\|\rho - \rho_n\|_{L^\infty(\partial D(\boldsymbol{y}))} \leq C n^{-k} \|\rho\|_{C^k(\partial D(\boldsymbol{y}))},$$

where ρ_n is obtained from the Nyström method with $n = 2j$ points for some $j \in \mathbb{N}$.

Proof. For a proof of this statement, see [41]. ∎

Thus, if the density ρ is even analytic, we arrive at the error estimate

$$\|\rho - \rho_n\|_{L^\infty(\partial D(\boldsymbol{y}))} \leq C \exp(-cn),$$

for some constants $C, c > 0$.

5. Higher-Order Quasi-Monte Carlo. In light of the recent development of higher-order quasi-Monte Carlo (QMC) methods, in particular so-called *interlaced polynomial lattice (IPL) rules* [14, 17, 29], and their application to problems in uncertainty quantification [15, 18, 27], we consider here the approximation of prior and posterior expectations by such deterministic QMC rules. IPL rules are adapted to the integrand function in a preprocessing step using the Component-by-Component (CBC) algorithm [44, 45], which requires as an input some bounds on the parametric derivatives of the integrand. By the analysis of the previous section, we have such bounds at our disposal.

We consider approximations of Z, Z' given in Theorem 1 and (6), respectively, where we assume a uniform prior distribution $\mu_0(\mathrm{d}\boldsymbol{y}) = \prod_{k=1}^{s} \mathrm{d}y_k$ on the truncated parameter sequence, which we denote here by $\boldsymbol{y}_{1:s}$. Given a collection $\mathcal{P}_N = \{\boldsymbol{y}_0, \dots, \boldsymbol{y}_{N-1}\} \subset [0,1]^s$ of QMC points in s dimensions, the QMC approximation $\mathcal{Q}_{N,s}$ of the prior mean of a function $g\colon U \to \mathbb{R}$ is given by

$$\mathbb{E}[g] = \int_U g(\boldsymbol{y})\,\mu(\mathrm{d}\boldsymbol{y}) \approx \mathcal{Q}_{N,s}[g] := \frac{1}{N}\sum_{n=0}^{N-1} g\Big(\boldsymbol{y}_n - \frac{\mathbf{1}}{2}\Big). \tag{29}$$

With the choices $g(\boldsymbol{y}) = \exp\big(-\Phi(\boldsymbol{y},\delta)\big)$ and $g(\boldsymbol{y}) = \phi\big(q(\boldsymbol{y})\big)\exp\big(-\Phi(\boldsymbol{y},\delta)\big)$, we obtain the integrals Z and Z', which we approximate with (29). The posterior mean is then simply given as the ratio $\mathbb{E}^{\mu^\delta}[\phi\circ q] = Z'/Z$, see Theorem 1.

5.1. Interlaced Polynomial Lattice Rules. To give the points $\boldsymbol{y}_n$, $n = 0,\dots,N-1$, we require some definitions and notation. A polynomial lattice rule (without interlacing) is a rule with $N = b^m$ points for some prime b and a positive integer m, and is given by a *generating vector* $\boldsymbol{q}$ whose components $q_j(x)$ are polynomials over the finite field $\mathbb{Z}_b$ of degree less than m. Let $\mathbb{Z}_b[x]$ denote the set of polynomials over $\mathbb{Z}_b$. We associate with each integer $n = 0,\dots,b^m-1$ a polynomial $n(x) = \sum_{k=0}^{m-1}\xi_k x^k$, where ξ_k are the digits of n in base b, that is $n = \xi_0 + \xi_1 b + \xi_2 b^2 + \ldots + \xi_{m-1}b^{m-1}$. To obtain points in $[0,1]$ from the generating vector $\boldsymbol{q}$, we require the mapping $v_m\colon \mathbb{Z}_b(x^{-1}) \to [0,1)$ given for integer w by

$$v_m\left(\sum_{k=w}^{\infty}\xi_k x^{-k}\right) = \sum_{k=\max(1,w)}^{m}\xi_k b^{-k}.$$

For an irreducible polynomial $P \in \mathbb{Z}_b[x]$ of degree m, the j-th component of the n-th point of the point set $\mathcal{P}_N$ is given by

$$(\boldsymbol{y}_n)_j = v_m\left(\frac{n(x)q_j(x)}{P(x)}\right).$$

To obtain orders of convergence higher than one, we consider an additional interlacing step. To this end, we denote the digit interlacing function of $\alpha \in \mathbb{N}$ points as $D_\alpha\colon [0,1)^\alpha \to [0,1)$,

$$D_\alpha(x_1,\dots,x_\alpha) = \sum_{a=1}^{\infty}\sum_{j=1}^{\alpha}\xi_{j,a}b^{-j-(a-1)\alpha},$$

where $\xi_{j,a}$ is the a-th digit in the expansion of the j-th point $x_j \in [0,1)$ in base b^{-1}, $x_j = \xi_{j,1}b^{-1} + \xi_{j,2}b^{-2} + \ldots$. For vectors in αs dimensions, digit interlacing is defined block-wise and denoted by $\mathcal{D}_\alpha\colon [0,1)^{\alpha s} \to [0,1)^s$ with

$$\mathcal{D}_\alpha(x_1,\dots,x_{\alpha s}) = \big(D_\alpha(x_1,\dots,x_\alpha), D_\alpha(x_{\alpha+1},\dots,x_{2\alpha}),\dots,D_\alpha(x_{(s-1)\alpha+1},\dots,x_{s\alpha})\big).$$

For a generating vector $\boldsymbol{q} \in (\mathbb{Z}_b[x])^{\alpha s}$ containing α components for each of the s dimensions, the interlaced polynomial lattice point set is $\mathcal{D}_\alpha(\widetilde{\mathcal{P}}_N) \subset [0,1)^s$, where $\widetilde{\mathcal{P}}_N \subset [0,1)^{\alpha s}$ denotes

the (classical) polynomial lattice point set in αs dimensions with generating vector $\boldsymbol{q}$. For more details on this method, see e.g. [14, 17, 29]. The following theorem states the higher order rates that are obtainable under suitable sparsity assumptions of the form stated in Section 2.

Proposition 19 (Thm. 3.1 from [17]). *For $m \geq 1$ and a prime b, let $N = b^m$ denote the number of QMC points. Let $s \geq 1$ and $\boldsymbol{\beta} = (\beta_j)_{j\geq 1}$ be a sequence of positive numbers, and let $\boldsymbol{\beta}_s = (\beta_j)_{1\leq j\leq s}$ denote the first s terms. Assume that $\boldsymbol{\beta} \in \ell^p(\mathbb{N})$ for some $p < 1$.*

If there exists a $c > 0$ such that a function F satisfies for $\alpha := \lfloor 1/p \rfloor + 1$ that

$$|(\partial_{\boldsymbol{y}}^{\boldsymbol{\nu}} F)(\boldsymbol{y})| \leq c\,|\boldsymbol{\nu}|!\,\boldsymbol{\beta}_s^{\boldsymbol{\nu}} \quad \text{for all } \boldsymbol{\nu} \in \{0, 1, \ldots, \alpha\}^s, s \in \mathbb{N}, \tag{30}$$

then an interlaced polynomial lattice rule of order α with N points can be constructed in $\mathcal{O}(\alpha\, s\, N \log N + \alpha^2\, s^2 N)$ operations, such that for the quadrature error holds

$$|I_s(F) - \mathcal{Q}_{N,s}(F)| \leq C_{\alpha,\boldsymbol{\beta},b,p}\, N^{-1/p}, \tag{31}$$

where the constant $C_{\alpha,\boldsymbol{\beta},b,p} < \infty$ is independent of s and N.

Note that by the previous proposition, the CBC algorithm used to obtain generating vectors for IPL rules scales quadratically in the number of dimensions s, and is thus not subject to the curse of dimensionality. The main ingredient in this method that allows higher-order convergence rates is digit interlacing, which is taken into account during the construction of the generating vector, cf. [17]. Numerical experiments detailing observations of such higher rates are given in [23, 27].

5.2. Combined Error Estimate. As mentioned in Section 2, we consider three approximations to the exact solution: dimension truncation, discretization of the partial differential equation (PDE), and quadrature approximation of the high-dimensional Bayesian integrals.

Combining Lemma 15 with (18) and considering the estimate (31) and Theorem 18, we obtain by the triangle inequality the following total error bound, where $p < 1$ denotes the summability of the sequence $\boldsymbol{\gamma}$ in a bound of the form (2) on the integrand function,

$$\left|I[\phi(q)] - \mathcal{Q}_N[\phi(q_n^{(s)})]\right| \leq C\left(s^{-\theta/p+1} + n^{-k} + N^{-1/p}\right),$$

where $C > 0$ is independent of the parametric dimension s, the number of discretization points n and the number of QMC points N. A similar combined error estimate is applied to a related model problem involving domain uncertainty in [23, Ch. 11.3] in the context of single-level and multilevel methods. There, the parameters N and s are chosen depending on the discretization error, which decreases on a suitably chosen hierarchy of finite element meshes.

5.3. Total Work. In the context of single-level and multilevel methods, an expression for the work required for evaluation of the approximation is required. Here, the total work of evaluating $\mathcal{Q}_N\left[\phi\left(q_n^{(s)}\right)\right]$ can be given in terms of the parameters N, s, and n by

$$W(N, s, n) = O(Nsn^3),$$

where $O(n^3)$ comes from the solution of a dense, $n \times n$ linear system of equations required in the boundary integral equation solver, which requires $O(s)$ work to compute each element of the matrix. This procedure is then repeated N times in the outer quadrature loop.

6. Numerical Experiments.

6.1. Setup. We consider the parametric problem (14) with the uncertain domain boundary $\Gamma(\omega)$ parametrized as described in Section 4. More precisely, we shall impose that the Karhunen-Loève expansion is given by a Fourier series with random coefficients, i.e.

$$u(\varphi,\omega) = u_0(\varphi) + \sigma \sum_{k=1}^{\infty} Y_k(\omega) u_k(\varphi).$$

Letting $Y_k \in [-1/2, 1/2]$ be uniformly distributed, we can identify the random variables $\{Y_k\}_k$ by their image $\boldsymbol{y} \in U = [-1/2, 1/2]^{\mathbb{N}}$. We additionally assume a constant nominal value $u_0(\varphi) \equiv u_0 \in (0,\infty)$ and write $u_{2k}(\varphi) = \vartheta_{2k}\cos(k\varphi)$ and $u_{2k-1} = \vartheta_{2k-1}\sin(k\varphi)$ yielding the parametric representation

$$u(\varphi,\boldsymbol{y}) = u_0 + \sigma \sum_{k=1}^{\infty} y_k u_k(\varphi), \tag{32}$$

where we choose throughout the following $u_0 = 0.3$, $\sigma = 0.125$ and $\vartheta_{2k} = \vartheta_{2k-1} = k^{-\zeta}$. The last choice enforces the decay $\sup_\varphi |u_k(\varphi)| \leq Ck^{-\zeta}$ where we choose $\zeta = 4$, implying that the unknown boundary Γ of the inclusion is at least four times continuously differentiable. We truncate the sum (32) at $s = 100$ terms, and are interested in the convergence of the QMC approximation to the resulting 100-dimensional integral with respect to the number of quadrature points. Assuming the dimension truncation error to converge like $\mathcal{O}(s^{-2/p+1})$, cf. Lemma 14, we have for $p = 1/\zeta = 1/4$ the behavior $\mathcal{O}(s^{-7})$. Letting this be of the order 10^{-14} to omit contributions of the dimension truncation error justifies the choice $s = 100$.

In the present context, considering the parametrization (21), we will be interested in computing prior ($\mu = \mu_0$) and posterior ($\mu = \mu^\delta$) expectation and variance,

$$\mathbb{E}^\mu[\Gamma(\boldsymbol{y})] = \big\{\mathbf{x} \in \mathbb{R}^2 : \mathbf{x} = \mathbb{E}^\mu[u(t,\boldsymbol{y})]\mathbf{e}(t),\ t \in I\big\} \tag{33}$$

$$\mathbb{V}^\mu[\Gamma(\boldsymbol{y})] = \big\{\mathbf{x} \in \mathbb{R}^2 : \mathbf{x} = \mathbb{V}^\mu[u(t,\boldsymbol{y})]\mathbf{e}(t),\ t \in I\big\}. \tag{34}$$

Based on the analysis in Section 2.2, we consider higher-order quasi-Monte Carlo with smoothness-driven product and order dependent (SPOD) weights, as introduced in [17]. For the experiments presented here, we used generating vectors constructed by the fast CBC method and made available in [28], with parameters $\alpha = \zeta$, sequence $\beta_j = \sigma\vartheta_j$, and Walsh coefficient bound $C = 0.1$. The construction was executed for $\zeta \in \{2,3,4\}$; see below for a discussion of the different cases. See also [27] for more computational details on CBC construction of IPL rules and the mentioned parameters. For the implementation, we used a custom boundary integral solver coupled with the `gMLQMC` library [22] for applying HOQMC.

As observation operator $\mathcal{O}$, we consider the evaluation of the solution's Neumann data $\partial q/\partial \mathbf{n}$ in $K = 16$ equi-spaced points (with respect to the angle) on the outer boundary Σ, and thus $\delta = \mathcal{O}(q) + \eta \in \mathbb{R}^{16}$. For smaller values of K, we expect the posterior to be less concentrated, yielding an "easier" integration problem. In the limit of large K, concentration effects similar to those in the small Γ limit arise, see below. We do not consider here the problem of experimental design, i.e. which evaluation points to choose or what the optimal

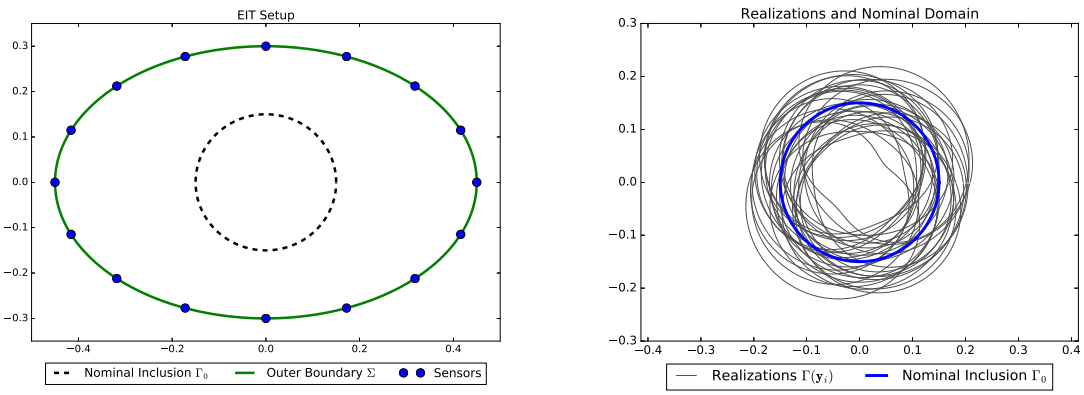

(a) (b)

Figure 2: a Simulation setup with outer boundary Σ, the nominal inner boundary Γ_0, and locations of the $K = 16$ sensors. b Realizations of the inclusion $\Gamma(\boldsymbol{y})$ resulting from the IPL point set with $m = 5$.

number of measurements might be, see e.g. [4, 5] for approaches related to experimental design in the Bayesian context.

As quantity of interest, we are interested in the interior boundary, which we represent as a vector of radius values of length M, for equispaced points in the angle φ. Thus, the QoI $\phi(q(\boldsymbol{y})) \in \mathbb{R}^M$ is, for each parameter vector $\boldsymbol{y}$, a discrete approximation of the shape of the inclusion. Figure 2 shows a setup of the experiment with the enclosing ellipse Σ (semiaxes 0.45 and 0.3), the nominal domain Γ_0, and various realizations of the parametric domain $\Gamma(\boldsymbol{y})$. Finally, the prescribed Dirichlet data at Σ are given by $g_{\mathrm{D}}(\mathbf{x}) = x_1^2 - x_2^2$.

6.2. Results. The prior and posterior expectations of the domain shape are given in Figure 3, which shows that incorporation of measurement data gives a reasonable estimate of the "true" shape. Moreover, the Bayesian framework allows specification of a confidence interval to assess the inherent uncertainty in the model and measurement process; in this example, the true shape is fully contained in the 1σ-confidence interval around the posterior mean, whereas the prior mean deviates significantly.

We are particularly interested in the verification of convergence rates of the approximations to the high-dimensional integrals Z and Z' from Theorem 1 and (6) using interlaced polynomial lattice rules (IPL). The prior expectation of the inclusion's shape in this case does not depend on the solution to the PDE (20); moreover, it is by the parametrization (23) simply an affine function of the parameters y_j. Prescribing a decay $\zeta = 4$, we thus expect due to (31) a convergence rate of N^{-4} for the prior expectation, for interlacing factor $\alpha = 4$. In the case where the QoI depends on the solution, the condition that the sequence of $W^{1,\infty}$-norms in γ_k from (12) is summable implies the loss of one order of convergence, which would imply the rate N^{-3} for the prior approximation, and the use of $\zeta = 3$ also in the CBC construction.

For the posterior, Theorem 4 implies an additional loss of one order of convergence; assuming the condition in (2) on the parameter-to-solution map $G\colon \boldsymbol{y} \to q(\boldsymbol{y};\cdot)$ for $1/\zeta < p < 1/3$, we thus obtain an expected higher-order QMC convergence rate of $N^{-\zeta+2}$. For the case of $\zeta = 4$ considered here, we thus expect N^{-2} when using IPL rules with interlacing factor $\alpha \geq 2$. We note that the generating vectors used in the posterior mean approximation were based on $\zeta = 2$ with interlacing factor $\alpha = 2$.

We consider both the prior and posterior expectations of the quantity of interest ϕ, which, as described above, yields a discrete approximation of the boundary $r_{\boldsymbol{y}}(\varphi)$ with M points $\varphi_1, \dots, \varphi_M$. We compute the error by approximating the L^2-norm over the angle φ, given for the prior by

$$\begin{aligned} \|(\mathbb{E}^{\mu_0} - \mathcal{Q}_N)[r_{\boldsymbol{y}}(\cdot)]\|^2_{L^2([0,2\pi])} &= \int_0^{2\pi} \Big(\mathbb{E}^{\mu_0}[r_{\boldsymbol{y}}(\varphi)] - \mathcal{Q}_N[r_{\boldsymbol{y}}(\varphi)]\Big)^2 \,\mathrm{d}\varphi \\ &\approx \frac{1}{M}\sum_{i=1}^{M} \Big(\mathbb{E}^{\mu_0}[r_{\boldsymbol{y}}(\varphi_i)] - \mathcal{Q}_N[r_{\boldsymbol{y}}(\varphi_i)]\Big)^2, \end{aligned} \tag{35}$$

and analogously for the posterior mean $\mathbb{E}^{\mu^\delta}$ over $\boldsymbol{y} \in U$. Due to the lack of an analytically given exact solution, we use a reference solution computed with $N = 2^{20}$ points using an interlaced polynomial lattice (IPL) rule, and consider in the following convergence plots the values $N = 2^k$ for $k = 1, \dots, 19$. As a comparison to IPL rules, we also compute Halton and "plain vanilla" Monte Carlo (MC) estimates of the involved integrals for the same values of N, where the expected convergence rates in this case are N^{-1} and $N^{-1/2}$, respectively. For MC, we approximate the L^2-error by averaging over $R = 10$ repetitions.

Figures 4 and 5 show the convergence of approximations to the prior and posterior expectation obtained using the methods mentioned above. A linear least squares fit is included to measure the convergence rate; the points used in the fit correspond to the points at which the linear fit is evaluated. Note that in Figure 4, the prior expectation does not involve the solution of the PDE, thus we obtain the full rate $N^{-\zeta}$. If the QoI were to depend on the solution $q(\boldsymbol{y})$, we would expect a rate $N^{-\zeta+1}$. In Figure 5, various values of the observation noise covariance Γ are considered.

For small Γ, concentration effects cause the performance of the methods to deteriorate, as is to be expected, see e.g. [49]. More precisely, assuming a unimodal posterior distribution, the posterior converges to a Dirac distribution as $\Gamma \to 0$. For small positive values of Γ, the region of parameter space where the posterior takes relatively large values (and thus the set of important parameters) decreases in size as Γ becomes smaller. For QMC approximation of the integral, this implies that many of the quadrature points lie in a region of parameter space which does not contribute significantly to the value of the integral. The expected IPL rate here is N^{-2}, which can be seen for large Γ in Figure 5.

7. Conclusion.

In this article we have described the application of higher-order quasi-Monte Carlo methods to a Bayesian approach for shape uncertainty quantification based on a parametric partial differential equation forward model. In particular, we have established a rigorous analysis of the posterior measure and a dimension truncation analysis for the forward model. This analysis supplements the results from [33] for diffusion problems on random

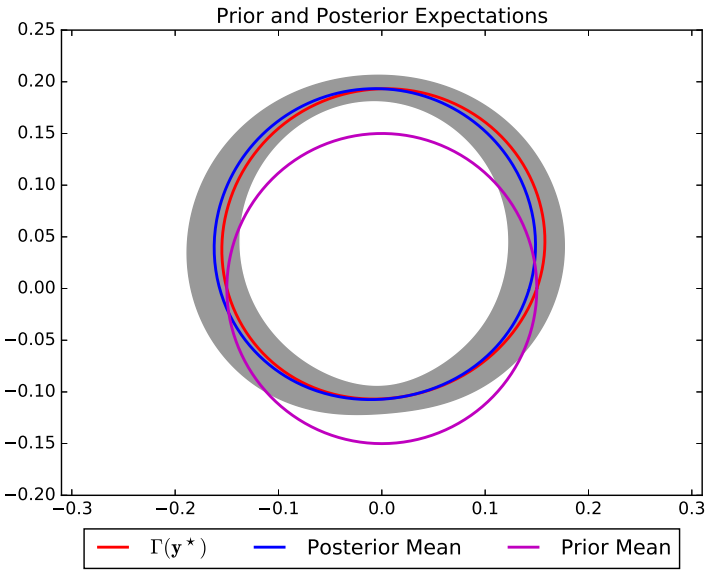

Figure 3: Prior and posterior expectations of the inclusion for $\Gamma = (0.1)^2$. The grey shaded area is a 1σ-confidence interval, which in this case contains the "truth" $\Gamma(\boldsymbol{y}^\star)$. It can be seen that the prior expectation deviates significantly from $\Gamma(\boldsymbol{y}^\star)$.

domains. The presented regularity analysis can be applied to any elliptic diffusion problem with a random coefficient. In particular, we have addressed the case of limited smoothness in the data. Furthermore, the article at hand covers the parameter estimation for the random vector field which is used to model random domains. The presented bounds on mixed partial derivatives of the posterior imply higher-order convergence rates of the quadrature error versus the number of nodes. The obtained convergence rates depend on the quantity of interest and choice of either prior or posterior measure. Numerical results conducted for an elliptic equation arising in Electrical Impedance Tomography confirm the theoretically derived rates in $s = 100$ parametric dimensions. A comparison with Halton and Monte Carlo sampling shows the superiority of the applied interlaced polynomial lattice rules in the case where the observation noise covariance is not too small.

Acknowledgments. We would like to thank Helmut Harbrecht and Christoph Schwab for suggesting the present analysis and for the fruitful discussions and many helpful remarks.

Appendix A. Multivariate Combinatorics. We start this section by defining the arithmetic for multi-indices. To that end, let $\boldsymbol{\alpha}, \boldsymbol{\beta} \in \mathbb{N}_0^s$ for some $s \in \mathbb{N}$. We define the addition and subtraction of two multi-indices in the canonical way. Moreover, we define

$$\boldsymbol{\alpha}^{\boldsymbol{\beta}} := \alpha_1^{\beta_1} \cdots \alpha_s^{\beta_s}$$

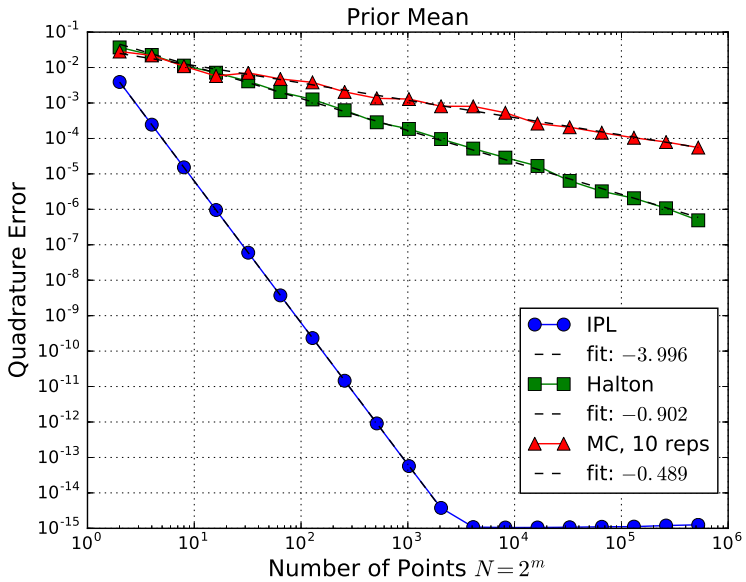

Figure 4: Approximations to the prior expectation with IPL, Halton and MC rules. The expected rates are N^{-4} for IPL, N^{-1} for Halton and $N^{-1/2}$ for MC, which are all confirmed by these results.

with the convention $0^0 = 1$. The modulus of $\boldsymbol{\alpha}$ is given by

$$|\boldsymbol{\alpha}| := \sum_{i=1}^{s} \alpha_i$$

and its factorial is defined according to

$$\boldsymbol{\alpha}! := \alpha_1! \cdots \alpha_s!.$$

Then, we can also define the multivariate binomial coefficient

$$\binom{\boldsymbol{\alpha}}{\boldsymbol{\beta}} := \frac{\boldsymbol{\alpha}!}{(\boldsymbol{\alpha}-\boldsymbol{\beta})!\boldsymbol{\beta}!},$$

where we assume $\boldsymbol{\beta} \leq \boldsymbol{\alpha}$ and the relation $\leq$ has to be understood component-wise.

The following lemma is a special case of formula (7.4) in [11].

Lemma 20. *Let $\boldsymbol{\gamma} = \{\gamma_k\}_k \in \ell^1(\mathbb{N})$ with $\gamma_k \geq 0$. Moreover, assume that $c_{\boldsymbol{\gamma}} := \|\boldsymbol{\gamma}\|_{\ell^1} < 1$. Then, it holds*

$$\sum_{\boldsymbol{\nu}} \frac{|\boldsymbol{\nu}|!}{\boldsymbol{\nu}!}\boldsymbol{\gamma}^{\boldsymbol{\nu}} = \frac{1}{1-c_{\boldsymbol{\gamma}}} \quad \text{for all } \boldsymbol{\nu} \in \mathcal{F}.$$

and therefore there exists a constant with $|\boldsymbol{\nu}|!/\boldsymbol{\nu}!\boldsymbol{\gamma}^{\boldsymbol{\nu}} \leq c$ for all $\boldsymbol{\nu} \in \mathcal{F}$.

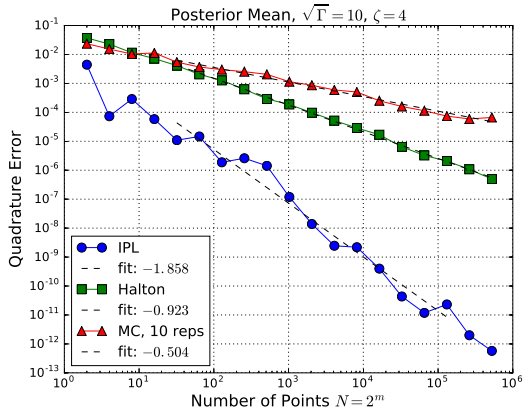

(a) $\Gamma = 10^2$.

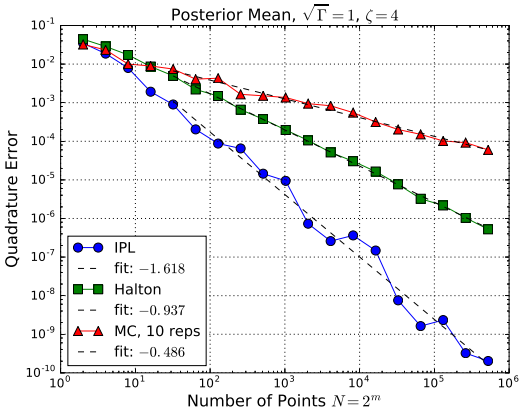

(b) $\Gamma = 1^2$.

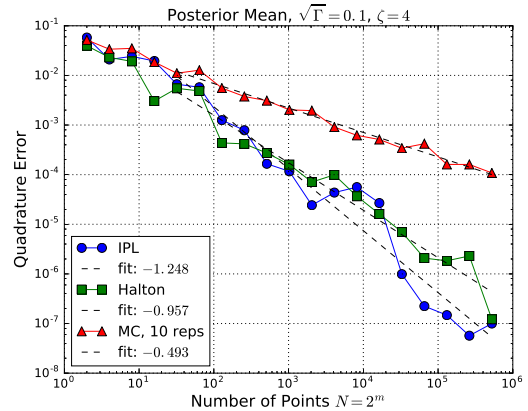

(c) $\Gamma = (0.1)^2$.

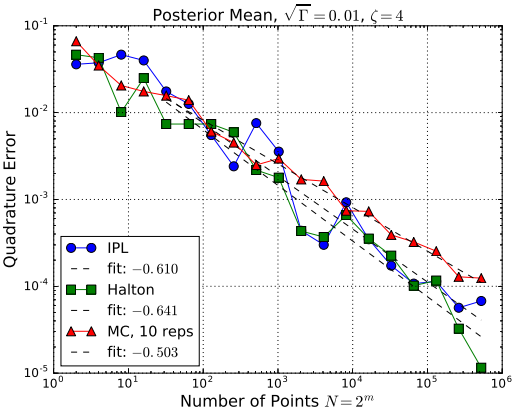

(d) $\Gamma = (0.01)^2$.

Figure 5: Convergence of IPL, Halton and MC approximations to the posterior expectation for different Γ, with the error computed as in (35) wrt. a reference solution with $N = 2^{20}$ IPL points.

Proof. Let $\mathcal{F}^{(s)} := \{\boldsymbol{\nu} \in \mathcal{F} : \nu_k = 0 \text{ for all } k > s\}$. Then, we have obviously $\mathcal{F} = \cup_{s\in\mathbb{N}}\mathcal{F}^{(s)}$. Now, there holds for all $\boldsymbol{\nu} \in \mathcal{F}^{(s)}$ that

$$\sum_{\boldsymbol{\nu}} \frac{|\boldsymbol{\nu}|!}{\boldsymbol{\nu}!}\boldsymbol{\gamma}^{\boldsymbol{\nu}} = \sum_{k=0}^{\infty}\sum_{|\boldsymbol{\nu}|=k}\frac{k!}{\boldsymbol{\nu}!}\boldsymbol{\gamma}^{\boldsymbol{\nu}} = \sum_{k=0}^{\infty}\left(\sum_{j=1}^{s}\gamma_j\right)^k \leq \sum_{k=0}^{\infty} c_{\boldsymbol{\gamma}}^k = \frac{1}{1-c_{\boldsymbol{\gamma}}}$$

by the multinomial theorem and the limit of the geometric series. Since the derived bound is uniform in the support size $s \in \mathbb{N}$ of the index sequences, we arrive at the assertion. ∎

Lemma 21. *For all $\alpha, \beta, r \in \mathbb{N}_0$ with $r > 0$ it holds*

$$\binom{\alpha+r-1}{r-1}\binom{\beta+r-1}{r-1} \leq \frac{(\alpha+\beta)!}{\alpha!\beta!}\binom{\alpha+\beta+r-1}{r-1}.$$

Proof. It holds

$$\begin{aligned}
&\binom{\alpha+r-1}{r-1}\binom{\beta+r-1}{r-1} \leq \frac{(\alpha+\beta)!}{\alpha!\beta!}\binom{\alpha+\beta+r-1}{r-1} \\
\iff\ &\binom{\alpha+r-1}{r-1}\frac{(\beta+r-1)!}{\beta!(r-1)!} \leq \frac{(\alpha+\beta)!}{\alpha!\beta!}\frac{(\alpha+\beta+r-1)!}{(\alpha+\beta)!(r-1)!} \\
\iff\ &\binom{\alpha+r-1}{r-1}(\beta+r-1)! \leq \frac{(\alpha+\beta+r-1)!}{\alpha!} \\
\iff\ &\binom{\alpha+r-1}{r-1} \leq \binom{\alpha+\beta+r-1}{\beta+r-1}.
\end{aligned}$$

The last inequality is true due to the monotonically increasing diagonals in Pascal's triangle. This proves the assertion. ∎

Lemma 22. *It holds for $\boldsymbol{\alpha} \in \mathbb{N}_0^s, \boldsymbol{\alpha}' \in \mathbb{N}_0^{s'}$ that*

$$\prod_{i=1}^{s}\binom{\alpha_i+|\boldsymbol{\alpha}'|-1}{|\boldsymbol{\alpha}'|-1} \leq \frac{|\boldsymbol{\alpha}|!}{\boldsymbol{\alpha}!}\binom{|\boldsymbol{\alpha}|+|\boldsymbol{\alpha}'|-1}{|\boldsymbol{\alpha}'|-1}.$$

Proof. The proof is by induction on s. For $s = 1$, we have

$$\binom{\alpha_1+|\boldsymbol{\alpha}'|-1}{|\boldsymbol{\alpha}'|-1} = \frac{\alpha_1!}{\alpha_1!}\binom{\alpha_1+|\boldsymbol{\alpha}'|-1}{|\boldsymbol{\alpha}'|-1},$$

which holds with equality. Let the induction hypothesis be valid for $s-1$ and set $\boldsymbol{\alpha}_{s-1} = [\alpha_1, \ldots, \alpha_{s-1}]$. Then, we derive with the previous lemma that

$$\begin{aligned}
\prod_{i=1}^{s}\binom{\alpha_i+|\boldsymbol{\alpha}'|-1}{|\boldsymbol{\alpha}'|-1} &\leq \frac{|\boldsymbol{\alpha}_{s-1}|!}{\boldsymbol{\alpha}_{s-1}!}\binom{|\boldsymbol{\alpha}_{s-1}|+|\boldsymbol{\alpha}'|-1}{|\boldsymbol{\alpha}'|-1}\binom{\alpha_s+|\boldsymbol{\alpha}'|-1}{r-1} \\
&\leq \frac{|\boldsymbol{\alpha}_{s-1}|!}{\boldsymbol{\alpha}_{s-1}!}\frac{(|\boldsymbol{\alpha}_{s-1}|+\alpha_s)!}{|\boldsymbol{\alpha}_{s-1}|!\alpha_s!}\binom{|\boldsymbol{\alpha}_{s-1}|+\alpha_s+|\boldsymbol{\alpha}'|-1}{|\boldsymbol{\alpha}'|-1} \\
&= \frac{|\boldsymbol{\alpha}|!}{\boldsymbol{\alpha}!}\binom{|\boldsymbol{\alpha}|+|\boldsymbol{\alpha}'|-1}{|\boldsymbol{\alpha}'|-1}.
\end{aligned}$$

∎

REFERENCES

[1] M. Abramowitz and I. A. Stegun, *Handbook of Mathematical Functions: With Formulas, Graphs, and Mathematical Tables*, Applied mathematics series, Dover Publications, N. Chemsford, MA, 1964.

[2] I. Akduman and R. Kress, *Electrostatic imaging via conformal mapping*, Inverse Problems, 18 (2002), pp. 1659–1672, doi:10.1088/0266-5611/18/6/315.

[3] G. Alessandrini, V. Isakov, and J. Powell, *Local uniqueness in the inverse conductivity problem with one measurement*, Trans. Amer. Math. Soc., 347 (1995), pp. 3031–3041, doi:10.2307/2154768.

[4] A. Alexanderian, P. J. Gloor, and O. Ghattas, *On Bayesian A- and D-optimal experimental designs in infinite dimensions*, Bayesian Anal., 11 (2016), pp. 671–695, doi:10.1214/15-BA969.

[5] A. Alexanderian, N. Petra, G. Stadler, and O. Ghattas, *A-optimal design of experiments for infinite-dimensional Bayesian linear inverse problems with regularized ℓ_0-sparsification*, SIAM J. Sci. Comput., 36 (2014), pp. A2122–A2148, doi:10.1137/130933381.

[6] J. Beck, R. Tempone, F. Nobile, and L. Tamellini, *On the optimal polynomial approximation of stochastic PDEs by Galerkin and collocation methods*, Math. Models Methods Appl. Sci., 22 (2012), pp. 1250023, 33, doi:10.1142/S0218202512500236.

[7] M. Brühl, *Explicit characterization of inclusions in electrical impedance tomography*, SIAM J. Math. Anal., 32 (2001), pp. 1327–1341, doi:10.1137/S003614100036656X.

[8] J. E. Castrillón-Candás, F. Nobile, and R. F. Tempone, *Analytic regularity and collocation approximation for elliptic PDEs with random domain deformations*, Comput. Math. Appl., 71 (2016), pp. 1173–1197, doi:10.1016/j.camwa.2016.01.005.

[9] R. Chapko and R. Kress, *A hybrid method for inverse boundary value problems in potential theory*, J. Inverse Ill-Posed Probl., 13 (2005), pp. 27–40, doi:10.1163/1569394053583711.

[10] P. Chen and C. Schwab, *Adaptive sparse grid model order reduction for fast Bayesian estimation and inversion*, in Sparse Grids and Applications - Stuttgart 2014, J. Garcke and D. Pflüger, eds., Cham, 2016, Springer International Publishing, pp. 1–27, doi:10.1007/978-3-319-28262-6_1.

[11] A. Cohen, R. DeVore, and C. Schwab, *Convergence rates of best N-term Galerkin approximations for a class of elliptic sPDEs*, Found. Comput. Math., 10 (2010), pp. 615–646, doi:10.1007/s10208-010-9072-2.

[12] G. M. Constantine and T. H. Savits, *A multivariate Faà di Bruno formula with applications*, Trans. Amer. Math. Soc., 348 (1996), pp. 503–520, doi:10.1090/S0002-9947-96-01501-2.

[13] M. Dashti and A. M. Stuart, *The Bayesian approach to inverse problems*, (to appear in Springer Handbook of Uncertainty Quantification), (2013), arXiv:1302.6989.

[14] J. Dick, *Walsh spaces containing smooth functions and quasi-Monte Carlo rules of arbitrary high order*, SIAM Journal on Numerical Analysis, 46 (2008), pp. 1519–1553, doi:10.1137/060666639.

[15] J. Dick, R. N. Gantner, Q. T. Le Gia, and C. Schwab, *Higher order quasi-Monte Carlo integration for Bayesian estimation*, Tech. Report 2016-13, Seminar for Applied Mathematics, ETH Zürich, Switzerland, 2016, https://www.sam.math.ethz.ch/sam_reports/reports_final/reports2016/2016-13.pdf.

[16] J. Dick, R. N. Gantner, Q. T. Le Gia, and C. Schwab, *Multilevel higher order quasi-Monte Carlo Bayesian estimation*, Tech. Report 2016-34, Seminar for Applied Mathematics, ETH Zürich, Switzerland, 2016, https://www.sam.math.ethz.ch/sam_reports/reports_final/reports2016/2016-34.pdf.

[17] J. Dick, F. Y. Kuo, Q. T. Le Gia, D. Nuyens, and C. Schwab, *Higher order QMC Petrov-Galerkin discretization for affine parametric operator equations with random field inputs*, SIAM Journal on Numerical Analysis, 52 (2014), p. 2676–2702, doi:10.1137/130943984.

[18] J. Dick, Q. T. Le Gia, and C. Schwab, *Higher order quasi–Monte Carlo integration for holomorphic, parametric operator equations*, SIAM/ASA Journal on Uncertainty Quantification, 4 (2016), p. 48–79, doi:10.1137/140985913.

[19] M. M. Dunlop and A. M. Stuart, *The Bayesian formulation of EIT: analysis and algorithms*, Inverse Probl. Imaging, 10 (2016), pp. 1007–1036, doi:10.3934/ipi.2016030.

[20] K. Eppler and H. Harbrecht, *A regularized Newton method in electrical impedance tomography using shape Hessian information*, Control Cybernet., 34 (2005), pp. 203–225.

[21] A. Friedman and V. Isakov, *On the uniqueness in the inverse conductivity problem with one measurement*, Indiana University Mathematics Journal, 38 (1989), pp. 563–579.

[22] R. N. Gantner, *A generic C++ library for multilevel quasi-Monte Carlo*, in Proceedings of the Platform for Advanced Scientific Computing Conference, PASC '16, New York, NY, USA, 2016, ACM, pp. 11:1–11:12, doi:10.1145/2929908.2929915.

[23] R. N. Gantner, *Computational Higher-Order Quasi-Monte Carlo for Random Partial Differential Equations*, PhD thesis, ETH Zürich, 2017.

[24] R. N. Gantner, *Dimension truncation in QMC for affine-parametric operator equations*, Tech. Report

2017-03, Seminar for Applied Mathematics, ETH Zürich, Switzerland, 2017, https://www.sam.math.ethz.ch/sam_reports/reports_final/reports2017/2017-03.pdf.

[25] R. N. Gantner, L. Herrmann, and C. Schwab, *Multilevel qmc with product weights for affine-parametric, elliptic pdes*, Tech. Report 2016-54, Seminar for Applied Mathematics, ETH Zürich, Switzerland, 2016, https://www.sam.math.ethz.ch/sam_reports/reports_final/reports2016/2016-54.pdf.

[26] R. N. Gantner, L. Herrmann, and Ch. Schwab, *Quasi-Monte Carlo integration for affine-parametric, elliptic PDEs: local supports and product weights*, Tech. Report 2016-32 (revised), Seminar for Applied Mathematics, ETH Zürich, Switzerland, 2016, https://www.sam.math.ethz.ch/sam_reports/reports_final/reports2016/2016-32_rev2.pdf.

[27] R. N. Gantner and C. Schwab, *Computational higher order quasi-Monte Carlo integration*, in Monte Carlo and Quasi-Monte Carlo Methods: MCQMC, Leuven, Belgium, April 2014, R. Cools and D. Nuyens, eds., Springer International Publishing, Cham, 2016, pp. 271–288, doi:10.1007/978-3-319-33507-0_12.

[28] R. N. Gantner and C. Schwab, *Generating vector repository*. http://www.sam.math.ethz.ch/HOQMC/genvecs/, 2016. Accessed: 2016-08-05.

[29] T. Goda and J. Dick, *Construction of interlaced scrambled polynomial lattice rules of arbitrary high order*, Foundations of Computational Mathematics. The Journal of the Society for the Foundations of Computational Mathematics, 15 (2015), pp. 1245–1278, doi:10.1007/s10208-014-9226-8.

[30] H. Harbrecht and T. Hohage, *A Newton method for reconstructing non star-shaped domains in electrical impedance tomography*, Inverse Probl. Imaging, 3 (2009), pp. 353–371, doi:10.3934/ipi.2009.3.353.

[31] H. Harbrecht and M. Peters, *Solution of free boundary problems in the presence of geometric uncertainties*, Preprint 2015-02, Mathematisches Institut, Universität Basel, (2015). to appear in Radon Series on Computational and Applied Mathematics, de Gruyter.

[32] H. Harbrecht, M. Peters, and M. Siebenmorgen, *Efficient approximation of random fields for numerical applications*, Numer. Linear Algebra Appl., 22 (2015), pp. 596–617, doi:10.1002/nla.1976.

[33] H. Harbrecht, M. Peters, and M. Siebenmorgen, *Analysis of the domain mapping method for elliptic diffusion problems on random domains*, Numer. Math., 134 (2016), pp. 823–856, doi:10.1007/s00211-016-0791-4.

[34] F. Hettlich and W. Rundell, *The determination of a discontinuity in a conductivity from a single boundary measurement*, Inverse Problems, 14 (1998), pp. 67–82, doi:10.1088/0266-5611/14/1/008.

[35] S. Heubach and T. Mansour, *Combinatorics of compositions and words*, Discrete Mathematics and its Applications (Boca Raton), CRC Press, Boca Raton, FL, 2010.

[36] E. Hille and R. S. Phillips, *Functional Analysis and Semi-Groups*, vol. 31, American Mathematical Society, Providence, 1957.

[37] R. Hiptmair and A. Paganini, *Shape optimization by pursuing diffeomorphisms*, Comput. Methods Appl. Math., 15 (2015), pp. 291–305, doi:10.1515/cmam-2015-0013, http://dx.doi.org/10.1515/cmam-2015-0013.

[38] V. H. Hoang, C. Schwab, and A. M. Stuart, *Complexity analysis of accelerated MCMC methods for Bayesian inversion*, Inverse Problems, 29 (2013), pp. 085010, 37, doi:10.1088/0266-5611/29/8/085010.

[39] D. S. Holder, *Electrical Impedance Tomography: Methods, History and Applications*, CRC Press, Boca Raton, 2004.

[40] R. B. Holmes, *Smoothness of certain metric projections on Hilbert space*, Trans. Amer. Math. Soc., 184 (1973), pp. 87–100, doi:10.2307/1996401.

[41] R. Kress, *Linear integral equations*, Vol. 82 of Applied Mathematical Sciences, Springer, New York, 2nd ed., 1999.

[42] F. Y. Kuo, C. Schwab, and I. H. Sloan, *Quasi-Monte Carlo methods for high-dimensional integration: the standard (weighted Hilbert space) setting and beyond*, ANZIAM J., 53 (2011), pp. 1–37, doi:10.1017/S1446181112000077.

[43] M. Loève, *Probability Theory. I+II*, no. 45 in Graduate Texts in Mathematics, Springer, New York, 4th ed., 1977.

[44] D. Nuyens and R. Cools, *Fast algorithms for component-by-component construction of rank-1 lattice rules in shift-invariant reproducing kernel Hilbert spaces*, Mathematics of Computation, 75 (2006), p. 903–920 (electronic), doi:10.1090/S0025-5718-06-01785-6.

[45] D. Nuyens and R. Cools, *Fast component-by-component construction, a reprise for different kernels*, in Monte Carlo and quasi-Monte Carlo methods 2004, Springer, Berlin, 2006, p. 373–387, doi:10.1007/3-540-31186-6_22.
[46] A. Paganini, S. Sargheini, R. Hiptmair, and C. Hafner, *Shape optimization of microlenses*, Optics Express, 23 (2015), p. 13099, doi:10.1364/OE.23.013099.
[47] S. A. Sauter and C. Schwab, *Boundary Element Methods*, Springer, Berlin-Heidelberg, 2011.
[48] C. Schillings and C. Schwab, *Sparsity in Bayesian inversion of parametric operator equations*, Inverse Problems, 30 (2014), pp. 065007, 30, doi:10.1088/0266-5611/30/6/065007.
[49] C. Schillings and C. Schwab, *Scaling limits in computational Bayesian inversion*, ESAIM: Mathematical Modelling and Numerical Analysis (to appear), (2016), doi:10.1051/m2an/2016005.
[50] C. Schwab and R. A. Todor, *Karhunen-Loève approximation of random fields by generalized fast multipole methods*, J. Comput. Phys., 217 (2006), pp. 100–122, doi:10.1016/j.jcp.2006.01.048.
[51] J. Simon, *Differentiation with respect to the domain in boundary value problems*, Numer. Funct. Anal. Optim., 2 (1980), pp. 649–687 (1981), doi:10.1080/01630563.1980.10120631.
[52] O. Steinbach, *Numerische Näherungsverfahren für Elliptische Randwertprobleme: Finite Elemente und Randelemente*, Advances in Numerical Mathematics, Vieweg+Teubner, Stuttgart-Leipzig-Wiesbaden, 2003.
[53] D. Xiu and D. M. Tartakovsky, *Numerical methods for differential equations in random domains*, SIAM J. Sci. Comput., 28 (2006), pp. 1167–1185, doi:10.1137/040613160.